along microtubules through the axon to the neuron cell body, where uncoating and replication of PV occur. A reconstituted experimental system with rat primary neurons was established in order to test the above hypothesis. Molecular imaging experiments indicated that endosomes carrying both PV and PVR undergo retrograde transport through the axons of the primary neurons (86); however, additional research is required to elucidate the mechanisms underlying the endocytosis of PV at synapses and the manner and location of PV replication in the neuron cell body.

PV REPLICATION IN THE CNS

Determinants of Neuron-Specific Infection

In the CNS, PV preferentially infects motor neurons in the anterior horn of the spinal cord and in neurons in the brain stem and motor cortex (7, 11). PV infection is not observed in other sites, including the occipital lobe of the cerebral cortex. Lytic replication of PV in the motor neurons results in a characteristic flaccid paralysis of the limbs. Similar pathology is observed in PVR tg mice. Neuron-specific infection in the CNS seems to be determined by the presence of PVR, because in situ hybridization experiments demonstrated that PVR mRNA expression is observed in neurons but not in glial cells in mice that express PVR with the natural PVR promoter (56, 100); PV infection is observed in glial cells when PVR is expressed in glial cells under the control of a ubiquitous promoter in mice (43). On the other hand, it remains unclear why PV preferentially infects a subset of neurons. Bodian hypothesized that the route of infection, the neuronal network connections, and the intrinsic resistance of some neurons to infection determine this specificity (7, 11).

Role of the IRES in Attenuation of Neurovirulence

Wild-type PV strains replicate more efficiently and produce more severe pathological lesions in the CNS than attenuated strains. The degree of neurovirulence in different virus strains appears to primarily depend on the ability of the virus to replicate in the CNS. There are multiple neurovirulence determinants in the PV genome (60, 88, 114), with strong neurovirulence determinants mapped in the 5′ NCR of all three PV strains. Comparative sequence analysis between the attenuated Sabin 3 strain and its neurovirulent revertants demonstrated that a key mutation at nucleotide position 472 leads to a neurovirulent phenotype (21). Molecular genetic analysis employing reverse genetics of PV type 1 showed that a relatively strong determinant of neurovirulence resides in the 5′ NCR of the viral RNA, especially nucleotide position 480 (49); a neurovirulence determinant in the PV type 2 genome has been identified at nucleotide position 481 (64). These nucleotide positions exist within the region corresponding to the IRES (31, 91). The results suggest that the neurovirulence levels of individual PV strains correspond with their IRES activities, that is, efficient translation initiation in the CNS. It is also known that translation initiation mediated by the IRES of attenuated strains is lower than that of virulent strains in neuroblastoma cell lines (32, 61). Therefore, it is considered that the attenuation phenotype of vaccine strains is due to a neuronal cell-specific translational defect; this translational defect constitutes a barrier specific for attenuated strains.

Possible Mechanism for IRES-Mediated Attenuation In Vivo

Several proteins that interact with the PV IRES have been identified (5, 16, 35, 41, 66, 81, 82, 92). One of these proteins, polypyrimidine tract-binding protein (PTB), has been shown to play an important role in the translational activity of the PV IRES (34, 92). Depletion of PTB from cellular extracts inhibits translation mediated by the PV IRES in a cell-free system (34, 41, 42), and overexpression of PTB in cultured cells enhances translation mediated by the PV IRES (26). Examination of the interaction of PTB with the PV IRES has demonstrated impaired binding by PTB on the Sabin IRES in comparison with the wt IRES (30, 82). Interestingly, CNS cells express PTB at very low levels but contain high levels of a neural or brain-enriched homolog of PTB, nPTB (51, 63, 65, 98).

Guest et al. (29) examined the interaction of the IRESs of PV type 3 virulent Leon strain and Sabin 3 strain with PTB and nPTB. PTB and nPTB were found to bind to a site directly adjacent to the attenuating mutation, and binding at this site was less efficient on the Sabin 3 IRES than on the Leon IRES. The translational activities mediated by the IRES elements of Leon and Sabin 3 were determined by electroporating a bicistronic construct that contained either the Sabin 3 or the Leon 5′ untranslated region into neural cells of a living chicken embryo spinal cord. Translation in the chicken embryo spinal cord mediated by the Sabin 3 IRES was less efficient than translation mediated by the Leon IRES and was rescued by overexpression of PTB, but not nPTB or other IRES *trans*-activating factors. These data suggest that tissue-specific expression of PTB coupled to a reduced binding of PTB on

the Sabin 3 IRES led to the virus' CNS-specific attenuation. Similarly, tissue-specific expression and differential RNA-binding properties of PTB and nPTB are important determinants of neurovirulence of the GDVII strain of Theiler's murine encephalomyelitis virus (97).

ROLE OF QUASISPECIES IN PV PATHOGENESIS

The quasispecies of PV plays an important role in PV pathogenesis (see Chapter 12). PV, as well as other RNA viruses, has a high error rate in RNA replication, and therefore each viral genome in the population differs from others by one or more mutations. In the presence of selective pressures, the quasispecies is presumed to provide an advantage to survival of the viral population as a whole, since some of the mutants contained in the population may be able to adapt to new environments (17, 18). Interestingly, a single point mutation in the RNA-dependent RNA polymerase (3D-G64S) determines the polymerase fidelity, and virus containing this mutation exhibits a reduced error rate (93) (see Chapter 13). The 3D-G64S mutant and wt virus showed few differences in growth kinetics in cultured cells that were not under selective pressure; however, when wt and mutant viruses were propagated in the presence of guanidine hydrochloride, the frequency of appearance of guanidine-resistant virus in the presence of guanidine hydrochloride was lower in the mutant virus (111). This result suggested that the fitness to a new environment was decreased as a result of the high fidelity of the polymerase. Surprisingly, the 3D-G64S virus showed reduced neurovirulence when inoculated by a peripheral route into PVR tg mice but was able to replicate in the CNS when inoculated directly into the CNS (95, 111). These results suggested that a diversity of the PV genome is necessary for adapting to different external conditions during virus dissemination into different parts of the body. A virus population with diverse genomes is likely to contain an individual viral genome that could be a source of a founder that fits well in new environments, while candidate viruses are not likely to be present in a homogeneous population. Pfeiffer and Kirkegaard (94) infected a mixture of tagged PV from the peripheral routes and showed that only a subset of members of the infected pool of virus reached the CNS, suggesting that only a small number of viruses survived and were selected in certain situations. This bottleneck effect was not observed when tagged PV was inoculated in the peripheral sites of PVR tg mice deficient in the type I IFN response (59), suggesting that the quasispecies is required during the dissemination of PV in order to evade the IFN response by the host. Additional studies are needed to elucidate the importance of quasispecies in the pathogenesis of poliomyelitis (see Chapter 12).

CONCLUDING REMARKS

We have summarized barriers against PV infection in the host and mechanisms by which PV passes through them. In the late 1980s, two important findings were made: identification of the PVR, with the subsequent development of PVR tg mice, and identification of the IRES. As a result of these two breakthroughs, investigations of the pathogenesis of PV infection in the whole organism made significant progress; however, many features related to the pathogenesis of PV-induced disease remain unknown. In order to better answer some of the many unsolved questions, knowledge of additional new mechanisms and concepts important in PV infection may be required.

There are several topics that remain poorly understood and could provide important additions to our understanding of PV pathogenesis. (i) The mechanisms by which PV invades two physical barriers, the GI tract and BBB, need to be elucidated, because it is difficult to explain this invasion simply on the basis of PVR-dependent infection. It may be that invasion of these barriers is mediated by transcytosis and that identification of a receptor for transcytosis, rather than the PVR (receptor for infection), mediates PV entry into the GI tract and BBB. (ii) It is not known why the IFN response occurs in a tissue-specific manner upon PV infection and why extraneural tissues are protected by this response while neural tissues are not. It may be that the IFN response varies because of the sensing mechanism for viral replication. Therefore, studies on the viral sensors and molecules that execute the IFN response following PV infection may answer these questions. (iii) It is not known why PV preferentially infects motor neurons in the spinal cord. It may be that an additional factor(s) that is present in other areas of the CNS inhibits PV infection. (iv) PV uses PVR when it reaches the parenchyma of the CNS by means of axonal transport. Although the structural transition of the PV virion is initiated by binding the PVR, uncoating of the virion does not occur during axonal transport but begins in the soma of the neurons. It is possible that the number of PVRs that bind the virion may determine the fate of the PV particle, i.e., a small number of PVRs that bind each virion may not be sufficient to result

in viral conformational change but may be able to induce endocytosis of the virus on the surface of synapses. Alternatively, a cellular factor(s) that inhibits viral uncoating could exist in the axon. If this were the case, the virus would need to be free from such a factor(s) before replicating in the neural cell body. (v) The role of the quasispecies in PV dissemination remains unclear and needs to be explored.

REFERENCES

1. **Aoki, J., S. Koike, I. Ise, Y. Sato-Yoshida, and A. Nomoto.** 1994. Amino acid residues on human poliovirus receptor involved in interaction with poliovirus. *J Biol. Chem.* **269**:8431–8438.
2. **Armstrong, C.** 1939. Successful transfer of Lansing strain of poliomyelitis virus from the cotton rat to the white mouse. *Public Health Rep.* **54**:2303–2305.
3. **Belnap, D. M., B. M. McDermott, Jr., D. J. Filman, N. Cheng, B. L. Trus, H. J. Zuccola, V. R. Racaniello, J. M. Hogle, and A. C. Steven.** 2000. Three-dimensional structure of poliovirus receptor bound to poliovirus. *Proc. Natl. Acad. Sci. USA* **97**: 73–78.
4. **Bernhardt, G., J. Harber, A. Zibert, M. deCrombrugghe, and E. Wimmer.** 1994. The poliovirus receptor: identification of domains and amino acid residues critical for virus binding. *Virology* **203**:344–356.
5. **Blyn, L. B., K. M. Swiderek, O. Richards, D. C. Stahl, B. L. Semler, and E. Ehrenfeld.** 1996. Poly(rC) binding protein 2 binds to stem-loop IV of the poliovirus RNA 5′ noncoding region: identification by automated liquid chromatography-tandem mass spectrometry. *Proc. Natl. Acad. Sci. USA* **93**: 11115–11120.
6. **Bodian, D.** 1955. Emerging concept of poliomyelitis infection. *Science* **122**:105–108.
7. **Bodian, D.** 1949. Histopathologic basis of clinical findings in poliomyelitis. *Am. J. Med.* **6**:563–578.
8. **Bodian, D.** 1959. Poliomyelitis: pathogenesis and histopathology, p. 479–518. *In* T. M. Rivers and F. L. Horsfall, Jr. (ed.), *Viral and Rickettsial Infections of Man*, vol. 3. J. B. Lippincott, Philadelphia, PA.
9. **Bodian, D.** 1956. Poliovirus in chimpanzee tissues after virus feeding. *Am. J. Hyg.* **64**:181–197.
10. **Bodian, D.** 1954. Viremia in experimental poliomyelitis. II. Viremia and the mechanism of the provoking effect of injections or trauma. *Am. J. Hyg.* **60**:358–370.
11. **Bodian, D., and A. Howe.** 1940. An experimental study of the role of neurons in the dissemination of poliomyelitis virus in the nervous system. *Brain* **63**:135–162.
12. **Brady, S. T.** 1991. Molecular motors in the nervous system. *Neuron* **7**:521–533.
13. **Couderc, T., T. Barzu, F. Horaud, and R. Crainic.** 1990. Poliovirus permissivity and specific receptor expression on human endothelial cells. *Virology* **174**:95–102.
14. **Coyne, C. B., K. S. Kim, and J. M. Bergelson.** 2007. Poliovirus entry into human brain microvascular cells requires receptor-induced activation of SHP-2. *EMBO J.* **26**:4016–4028.
15. **Crotty, S., L. Hix, L. J. Sigal, and R. Andino.** 2002. Poliovirus pathogenesis in a new poliovirus receptor transgenic mouse model: age-dependent paralysis and a mucosal route of infection. *J. Gen. Virol.* **83**:1707–1720.
16. **del Angel, R. M., A. G. Papavassiliou, C. Fernandez-Tomas, S. J. Silverstein, and V. R. Racaniello.** 1989. Cell proteins bind to multiple sites within the 5′ untranslated region of poliovirus RNA. *Proc. Natl. Acad. Sci. USA* **86**:8299–8303.
17. **Domingo, E., and J. J. Holland.** 1997. RNA virus mutations and fitness for survival. *Annu. Rev. Microbiol.* **51**:151–178.
18. **Domingo, E., L. Menendez-Arias, and J. J. Holland.** 1997. RNA virus fitness. *Rev. Med. Virol.* **7**:87–96.
19. **Dragunsky, E., T. Nomura, K. Karpinski, J. Furesz, D. J. Wood, Y. Pervikov, S. Abe, T. Kurata, O. Vanloocke, G. Karganova, R. Taffs, A. Heath, A. Ivshina, and I. Levenbook.** 2003. Transgenic mice as an alternative to monkeys for neurovirulence testing of live oral poliovirus vaccine: validation by a WHO collaborative study. *Bull. W. H. O.* **81**:251–260.
20. **Enders, J. F., T. H. Weller, and F. C. Robbins.** 1949. Cultivation of the Lansing strain of poliomyelitis virus in cultures of various human embryonic tissues. *Science* **109**:85–87.
21. **Evans, D. M., G. Dunn, P. D. Minor, G. C. Schild, A. J. Cann, G. Stanway, J. W. Almond, K. Currey, and J. V. Maizel, Jr.** 1985. Increased neurovirulence associated with a single nucleotide change in a noncoding region of the Sabin type 3 poliovaccine genome. *Nature* **314**:548–550.
22. **Freistadt, M. S., G. Kaplan, and V. R. Racaniello.** 1990. Heterogeneous expression of poliovirus receptor-related proteins in human cells and tissues. *Mol. Cell. Biol.* **10**:5700–5706.
23. **Freistadt, M. S., and V. R. Racaniello.** 1991. Mutational analysis of the cellular receptor for poliovirus. *J. Virol.* **65**:3873–3876.
24. **Garcia-Sastre, A., R. K. Durbin, H. Zheng, P. Palese, R. Gertner, D. E. Levy, and J. E. Durbin.** 1998. The role of interferon in influenza virus tissue tropism. *J. Virol.* **72**:8550–8558.
25. **Goldstein, G. W., and A. L. Betz.** 1986. The blood-brain barrier. *Sci. Am.* **255**:74–83.
26. **Gosert, R., K. H. Chang, R. Rijnbrand, M. Yi, D. V. Sangar, and S. M. Lemon.** 2000. Transient expression of cellular polypyrimidine-tract binding protein stimulates cap-independent translation directed by both picornaviral and flaviviral internal ribosome entry sites in vivo. *Mol. Cell. Biol.* **20**:1583–1595.
27. **Gromeier, M., L. Alexander, and E. Wimmer.** 1996. Internal ribosomal entry site substitution eliminates neurovirulence in intergeneric poliovirus recombinants. *Proc. Natl. Acad. Sci. USA* **93**:2370–2375.
28. **Gromeier, M., and E. Wimmer.** 1998. Mechanism of injury-provoked poliomyelitis. *J. Virol.* **72**:5056–5060.
29. **Guest, S., E. Pilipenko, K. Sharma, K. Chumakov, and R. P. Roos.** 2004. Molecular mechanisms of attenuation of the Sabin strain of poliovirus type 3. *J. Virol.* **78**:11097–11107.
30. **Gutierrez, A. L., M. Denova-Ocampo, V. R. Racaniello, and R. M. del Angel.** 1997. Attenuating mutations in the poliovirus 5′ untranslated region alter its interaction with polypyrimidine tract-binding protein. *J. Virol.* **71**:3826–3833.
31. **Haller, A. A., J. H. Nguyen, and B. L. Semler.** 1993. Minimum internal ribosome entry site required for poliovirus infectivity. *J. Virol.* **67**:7461–7471.
32. **Haller, A. A., S. R. Stewart, and B. L. Semler.** 1996. Attenuation stem-loop lesions in the 5′ noncoding region of poliovirus RNA: neuronal cell-specific translation defects. *J. Virol.* **70**: 1467–1474.
33. **He, Y., V. D. Bowman, S. Mueller, C. M. Bator, J. Bella, X. Peng, T. S. Baker, E. Wimmer, R. J. Kuhn, and M. G. Rossmann.** 2000. Interaction of the poliovirus receptor with poliovirus. *Proc. Natl. Acad. Sci. USA* **97**:79–84.
34. **Hellen, C. U., T. V. Pestova, M. Litterst, and E. Wimmer.** 1994. The cellular polypeptide p57 (pyrimidine tract-binding protein) binds to multiple sites in the poliovirus 5′ nontranslated region. *J. Virol.* **68**:941–950.
35. **Hellen, C. U., G. W. Witherell, M. Schmid, S. H. Shin, T. V. Pestova, A. Gil, and E. Wimmer.** 1993. A cytoplasmic 57-kDa protein that is required for translation of picornavirus RNA

by internal ribosomal entry is identical to the nuclear pyrimidine tract-binding protein. *Proc. Natl. Acad. Sci. USA* 90: 7642–7646.

36. **Holland, J. J.** 1961. Receptor affinities as major determinants of enterovirus tissue tropisms in humans. *Virology* 15:312–326.
37. **Holland, J. J., L. McLaren, and J. T. Syverton.** 1959. Mammalian cell-virus relationship. III. Poliovirus production by nonprimate cells exposed to poliovirus ribonucleic acid. *Proc. Soc. Exp. Biol. Med.* 100:843–845.
38. **Holland, J. J., L. McLaren, and J. T. Syverton.** 1959. The mammalian cell-virus relationship. IV. Infection of naturally insusceptible cells with enterovirus ribonucleic acid. *J. Exp. Med.* 110:65–80.
39. **Horstmann, D. M., J. L. Melnick, R. Ward, and J. S. Fleitas.** 1947. The susceptibility of infant rhesus monkeys to poliomyelitis virus administered by mouth A study of the distribution of virus in the tissues of orally infected animals. *J. Exp. Med.* 86:309–323.
40. **Hsiung, G.-D., F. L. Black, and J. R. Henderson.** 1964. Susceptibility of primates to viruses in relation to taxonomic classification, p. 1–23. *In* J. Buettner-Jaenusch (ed.), *Evolutionary and Genetic Biology of Primates*, vol. 2. Academic Press, New York, NY.
41. **Hunt, S. L., J. J. Hsuan, N. Totty, and R. J. Jackson.** 1999. unr, a cellular cytoplasmic RNA-binding protein with five cold-shock domains, is required for internal initiation of translation of human rhinovirus RNA. *Genes Dev.* 13:437–448.
42. **Hunt, S. L., and R. J. Jackson.** 1999. Polypyrimidine-tract binding protein (PTB) is necessary, but not sufficient, for efficient internal initiation of translation of human rhinovirus-2 RNA. *RNA* 5:344–359.
43. **Ida-Hosonuma, M., T. Iwasaki, C. Taya, Y. Sato, J. Li, N. Nagata, H. Yonekawa, and S. Koike.** 2002. Comparison of neuropathogenicity of poliovirus in two transgenic mouse strains expressing human poliovirus receptor with different distribution patterns. *J. Gen. Virol.* 83:1095–1105.
44. **Ida-Hosonuma, M., T. Iwasaki, T. Yoshikawa, N. Nagata, Y. Sato, T. Sata, M. Yoneyama, T. Fujita, C. Taya, H. Yonekawa, and S. Koike.** 2005. The alpha/beta interferon response controls tissue tropism and pathogenicity of poliovirus. *J. Virol.* 79:4460–4469.
45. **Ida-Hosonuma, M., Y. Sasaki, H. Toyoda, A. Nomoto, O. Gotoh, H. Yonekawa, and S. Koike.** 2003. Host range of poliovirus is restricted to simians because of a rapid sequence change of the poliovirus receptor gene during evolution. *Arch. Virol.* 148:29–44.
46. **Iwasaki, A., R. Welker, S. Mueller, M. Linehan, A. Nomoto, and E. Wimmer.** 2002. Immunofluorescence analysis of poliovirus receptor expression in Peyer's patches of humans, primates, and CD155 transgenic mice: implications for poliovirus infection. *J. Infect. Dis.* 186:585–592.
47. **Kanamitsu, M., A. Kasamaki, M. Ogawa, S. Kasahara, and M. Imamura.** 1967. Immunofluorescent study on the pathogenesis of oral infection of poliovirus in monkeys. *Jpn. J. Med. Sci. Biol.* 20:175–194.
48. **Kauder, S. E., and V. R. Racaniello.** 2004. Poliovirus tropism and attenuation are determined after internal ribosome entry. *J. Clin. Investig.* 113:1743–1753.
49. **Kawamura, N., M. Kohara, S. Abe, T. Komatsu, K. Tago, M. Arita, and A. Nomoto.** 1989. Determinants in the 5′ noncoding region of poliovirus Sabin 1 RNA that influence the attenuation phenotype. *J. Virol.* 63:1302–1309.
50. **Khan, S., X. Peng, J. Yin, P. Zhang, and E. Wimmer.** 2008. Characterization of the New World monkey homologues of human poliovirus receptor CD155. *J. Virol.* 82:7167–7179.
51. **Kikuchi, T., M. Ichikawa, J. Arai, H. Tateiwa, L. Fu, K. Higuchi, and N. Yoshimura.** 2000. Molecular cloning and characterization of a new neuron-specific homologue of rat polypyrimidine tract binding protein. *J. Biochem.* 128:811–821.
52. **Koike, S., J. Aoki, and A. Nomoto.** 1994. Transgenic mouse model for the study of poliovirus pathogenesis, p. 463–480. *In* E. Wimmer and R. Weiss (ed.), *Receptor-Mediated Virus Entry into Cells*. Cold Spring Harbor Laboratory Press, Cold Spring Harbor, NY.
53. **Koike, S., H. Horie, I. Ise, A. Okitsu, M. Yoshida, N. Iizuka, K. Takeuchi, T. Takegami, and A. Nomoto.** 1990. The poliovirus receptor protein is produced both as membrane-bound and secreted forms. *EMBO J.* 9:3217–3224.
54. **Koike, S., I. Ise, and A. Nomoto.** 1991. Functional domains of the poliovirus receptor. *Proc. Natl. Acad. Sci. USA* 88:4104–4108.
55. **Koike, S., I. Ise, Y. Sato, H. Yonekawa, O. Gotoh, and A. Nomoto.** 1992. A second gene for the African green monkey poliovirus receptor that has no putative N-glycosylation site in the functional N-terminal immunoglobulin-like domain. *J. Virol.* 66:7059–7066.
56. **Koike, S., C. Taya, J. Aoki, Y. Matsuda, I. Ise, H. Takeda, T. Matsuzaki, H. Amanuma, H. Yonekawa, and A. Nomoto.** 1994. Characterization of three different transgenic mouse lines that carry human poliovirus receptor gene: influence of the transgene expression on pathogenesis. *Arch. Virol.* 139: 351–363.
57. **Koike, S., C. Taya, T. Kurata, S. Abe, I. Ise, H. Yonekawa, and A. Nomoto.** 1991. Transgenic mice susceptible to poliovirus. *Proc. Natl. Acad. Sci. USA* 88:951–955.
58. **Kunin, C. M., and W. S. Jordan, Jr.** 1961. In vitro absorption of poliovirus by noncultured tissues. Effect of species, age and malignancy. *Am. J. Hyg.* 73:245–257.
59. **Kuss, S. K., C. A. Etheredge, and J. K. Pfeiffer.** 2008. Multiple host barriers restrict poliovirus trafficking in mice. *PLoS Pathog.* 4:e1000082.
60. **La Monica, N., J. W. Almond, and V. R. Racaniello.** 1987. A mouse model for poliovirus neurovirulence identifies mutations that attenuate the virus for humans. *J. Virol.* 61:2917–2920.
61. **La Monica, N., and V. R. Racaniello.** 1989. Differences in replication of attenuated and neurovirulent polioviruses in human neuroblastoma cell line SH-SY5Y. *J. Virol.* 63:2357–2360.
62. **Landsteiner, K., and E. Popper.** 1908. Microscopische präparate von einem menschlichen und zwei affentückermarker. *Wein. Klin. Wochenschr.* 21:1930.
63. **Lillevali, K., A. Kulla, and T. Ord.** 2001. Comparative expression analysis of the genes encoding polypyrimidine tract binding protein (PTB) and its neural homologue (brPTB) in prenatal and postnatal mouse brain. *Mech. Dev.* 101:217–220.
64. **Macadam, A. J., S. R. Pollard, G. Ferguson, G. Dunn, R. Skuce, J. W. Almond, and P. D. Minor.** 1991. The 5′ noncoding region of the type 2 poliovirus vaccine strain contains determinants of attenuation and temperature sensitivity. *Virology* 181:451–458.
65. **Markovtsov, V., J. M. Nikolic, J. A. Goldman, C. W. Turck, M. Y. Chou, and D. L. Black.** 2000. Cooperative assembly of an hnRNP complex induced by a tissue-specific homolog of polypyrimidine tract binding protein. *Mol. Cell. Biol.* 20: 7463–7479.
66. **Meerovitch, K., J. Pelletier, and N. Sonenberg.** 1989. A cellular protein that binds to the 5′-noncoding region of poliovirus RNA: implications for internal translation initiation. *Genes Dev.* 3:1026–1034.
67. **Mendelsohn, C., B. Johnson, K. A. Lionetti, P. Nobis, E. Wimmer, and V. R. Racaniello.** 1986. Transformation of a human

poliovirus receptor gene into mouse cells. *Proc. Natl. Acad. Sci. USA* 83:7845–7849.

68. **Mendelsohn, C. L., E. Wimmer, and V. R. Racaniello.** 1989. Cellular receptor for poliovirus: molecular cloning, nucleotide sequence, and expression of a new member of the immunoglobulin superfamily. *Cell* 56:855–865.
69. **Miller, D. A., O. J. Miller, V. G. Dev, S. Hashmi, R. Tantravahi, L. Medrano, and H. Green.** 1974. Human chromosome 19 carries a poliovirus receptor gene. *Cell* 1:161–173.
70. **Morrison, M. E., Y. J. He, M. W. Wien, J. M. Hogle, and V. R. Racaniello.** 1994. Homolog-scanning mutagenesis reveals poliovirus receptor residues important for virus binding and replication. *J. Virol.* 68:2578–2588.
71. **Mrkic, B., J. Pavlovic, T. Rulicke, P. Volpe, C. J. Buchholz, D. Hourcade, J. P. Atkinson, A. Aguzzi, and R. Cattaneo.** 1998. Measles virus spread and pathogenesis in genetically modified mice. *J. Virol.* 72:7420–7427.
72. **Mueller, S., X. Cao, R. Welker, and E. Wimmer.** 2002. Interaction of the poliovirus receptor CD155 with the dynein light chain Tctex-1 and its implication for poliovirus pathogenesis. *J. Biol. Chem.* 277:7897–7904.
73. **Mueller, S., E. Wimmer, and J. Cello.** 2005. Poliovirus and poliomyelitis: a tale of guts, brains, and an accidental event. *Virus Res.* 111:175–193.
74. **Muller, U., U. Steinhoff, L. F. Reis, S. Hemmi, J. Pavlovic, R. M. Zinkernagel, and M. Aguet.** 1994. Functional role of type I and type II interferons in antiviral defense. *Science* 264:1918–1921.
75. **Nagata, N., T. Iwasaki, Y. Ami, Y. Sato, I. Hatano, A. Harashima, Y. Suzaki, T. Yoshii, T. Hashikawa, T. Sata, Y. Horiuchi, S. Koike, T. Kurata, and A. Nomoto.** 2004. A poliomyelitis model through mucosal infection in transgenic mice bearing human poliovirus receptor, TgPVR21. *Virology* 321:87–100.
76. **Nathanson, N.** 2008. The pathogenesis of poliomyelitis: what we don't know. *Adv. Virus Res.* 71:1–50.
77. **Nathanson, N., and D. Bodian.** 1961. Experimental poliomyelitis following intramuscular virus injection. I. The effect of neural block on a neurotropic and a pantropic strain. *Bull. Johns Hopkins Hosp.* 108:308–319.
78. **Nathanson, N., and A. D. Langmuir.** 1963. The Cutter incident. Poliomyelitis following formaldehyde-inactivated poliovirus vaccination in the United States during the spring of 1955. II. Relationship of poliomyelitis to Cutter vaccine. *Am. J. Hyg.* 78:29–60.
79. **Neutra, M. R., E. Pringault, and J. P. Kraehenbuhl.** 1996. Antigen sampling across epithelial barriers and induction of mucosal immune responses. *Annu. Rev. Immunol.* 14:275–300.
80. **Nobis, P., R. Zibirre, G. Meyer, J. Kuhne, G. Warnecke, and G. Koch.** 1985. Production of a monoclonal antibody against an epitope on HeLa cells that is the functional poliovirus binding site. *J. Gen. Virol.* 66:2563–2569.
81. **Ochs, K., L. Saleh, G. Bassili, V. H. Sonntag, A. Zeller, and M. Niepmann.** 2002. Interaction of translation initiation factor eIF4B with the poliovirus internal ribosome entry site. *J. Virol.* 76:2113–2122.
82. **Ochs, K., A. Zeller, L. Saleh, G. Bassili, Y. Song, A. Sonntag, and M. Niepmann.** 2003. Impaired binding of standard initiation factors mediates poliovirus translation attenuation. *J. Virol.* 77:115–122.
83. **Ohka, S., H. Igarashi, N. Nagata, M. Sakai, S. Koike, T. Nochi, H. Kiyono, and A. Nomoto.** 2007. Establishment of a poliovirus oral infection system in human poliovirus receptor-expressing transgenic mice that are deficient in alpha/beta interferon receptor. *J. Virol.* 81:7902–7912.
84. **Ohka, S., N. Matsuda, K. Tohyama, T. Oda, M. Morikawa, S. Kuge, and A. Nomoto.** 2004. Receptor (CD155)-dependent endocytosis of poliovirus and retrograde axonal transport of the endosome. *J. Virol.* 78:7186–7198.
85. **Ohka, S., and A. Nomoto.** 2001. Recent insights into poliovirus pathogenesis. *Trends Microbiol.* 9:501–506.
86. **Ohka, S., M. Sakai, S. Bohnert, H. Igarashi, K. Deinhardt, G. Schiavo, and A. Nomoto.** 2009. Receptor-dependent and -independent axonal retrograde transport of poliovirus in motor neurons. *J. Virol.* 83:4995–5004.
87. **Ohka, S., W. X. Yang, E. Terada, K. Iwasaki, and A. Nomoto.** 1998. Retrograde transport of intact poliovirus through the axon via the fast transport system. *Virology* 250:67–75.
88. **Omata, T., M. Kohara, S. Kuge, T. Komatsu, S. Abe, B. L. Semler, A. Kameda, H. Itoh, M. Arita, E. Wimmer, et al.** 1986. Genetic analysis of the attenuation phenotype of poliovirus type 1. *J. Virol.* 58:348–358.
89. **Ouzilou, L., E. Caliot, I. Pelletier, M. C. Prevost, E. Pringault, and F. Colbere-Garapin.** 2002. Poliovirus transcytosis through M-like cells. *J. Gen. Virol.* 83:2177–2182.
90. **Owen, R. L., and A. L. Jones.** 1974. Epithelial cell specialization within human Peyer's patches: an ultrastructural study of intestinal lymphoid follicles. *Gastroenterology* 66:189–203.
91. **Pelletier, J., and N. Sonenberg.** 1988. Internal initiation of translation of eukaryotic mRNA directed by a sequence derived from poliovirus RNA. *Nature* 334:320–325.
92. **Pestova, T. V., C. U. Hellen, and E. Wimmer.** 1991. Translation of poliovirus RNA: role of an essential *cis*-acting oligopyrimidine element within the 5′ nontranslated region and involvement of a cellular 57-kilodalton protein. *J. Virol.* 65: 6194–6204.
93. **Pfeiffer, J. K., and K. Kirkegaard.** 2003. A single mutation in poliovirus RNA-dependent RNA polymerase confers resistance to mutagenic nucleotide analogs via increased fidelity. *Proc. Natl. Acad. Sci. USA* 100:7289–7294.
94. **Pfeiffer, J. K., and K. Kirkegaard.** 2006. Bottleneck-mediated quasispecies restriction during spread of an RNA virus from inoculation site to brain. *Proc. Natl. Acad. Sci. USA* 103: 5520–5525.
95. **Pfeiffer, J. K., and K. Kirkegaard.** 2005. Increased fidelity reduces poliovirus fitness and virulence under selective pressure in mice. *PLoS Pathog.* 1:e11.
96. **Pilipenko, E. V., T. V. Pestova, V. G. Kolupaeva, E. V. Khitrina, A. N. Poperechnaya, V. I. Agol, and C. U. Hellen.** 2000. A cell cycle-dependent protein serves as a template-specific translation initiation factor. *Genes Dev.* 14:2028–2045.
97. **Pilipenko, E. V., E. G. Viktorova, E. V. Khitrina, S. V. Maslova, N. Jarousse, M. Brahic, and V. I. Agol.** 1999. Distinct attenuation phenotypes caused by mutations in the translational starting window of Theiler's murine encephalomyelitis virus. *J. Virol.* 73:3190–3196.
98. **Polydorides, A. D., H. J. Okano, Y. Y. Yang, G. Stefani, and R. B. Darnell.** 2000. A brain-enriched polypyrimidine tract-binding protein antagonizes the ability of Nova to regulate neuron-specific alternative splicing. *Proc. Natl. Acad. Sci. USA* 97:6350–6355.
99. **Racaniello, V. R.** 2006. One hundred years of poliovirus pathogenesis. *Virology* 344:9–16.
100. **Ren, R., and V. R. Racaniello.** 1992. Human poliovirus receptor gene expression and poliovirus tissue tropism in transgenic mice. *J. Virol.* 66:296–304.
101. **Ren, R., and V. R. Racaniello.** 1992. Poliovirus spreads from muscle to the central nervous system by neural pathways. *J. Infect. Dis.* 166:747–752.
102. **Ren, R. B., F. Costantini, E. J. Gorgacz, J. J. Lee, and V. R. Racaniello.** 1990. Transgenic mice expressing a human poliovirus receptor: a new model for poliomyelitis. *Cell* 63: 353–362.

103. **Ryman, K. D., W. B. Klimstra, K. B. Nguyen, C. A. Biron, and R. E. Johnston.** 2000. Alpha/beta interferon protects adult mice from fatal Sindbis virus infection and is an important determinant of cell and tissue tropism. *J. Virol.* **74:** 3366–3378.

104. **Sabin, A., and L. Boulger.** 1973. History of Sabin attenuated poliovirus oral live vaccine strains. *J. Biol. Stand.* **1:**115–118.

105. **Sabin, A. B.** 1965. Oral poliovirus vaccine. History of its development and prospects for eradication of poliomyelitis. *JAMA* **194:**872–876.

106. **Sabin, A. B.** 1956. Pathogenesis of poliomyelitis; reappraisal in the light of new data. *Science* **123:**1151–1157.

107. **Salk, J. E.** 1953. Principles of immunization as applied to poliomyelitis and influenza. *Am. J. Public Health Nations Health* **43:**1384–1398.

108. **Selinka, H. C., A. Zibert, and E. Wimmer.** 1991. Poliovirus can enter and infect mammalian cells by way of an intercellular adhesion molecule 1 pathway. *Proc. Natl. Acad. Sci. USA* **88:**3598–3602.

109. **Sicinski, P., J. Rowinski, J. B. Warchol, Z. Jarzabek, W. Gut, B. Szczygiel, K. Bielecki, and G. Koch.** 1990. Poliovirus type 1 enters the human host through intestinal M cells. *Gastroenterology* **98:**56–58.

110. **Takahashi, Y., S. Misumi, A. Muneoka, M. Masuyama, H. Tokado, K. Fukuzaki, N. Takamune, and S. Shoji.** 2008. Nonhuman primate intestinal villous M-like cells: an effective poliovirus entry site. *Biochem. Biophys. Res. Commun.* **368:**501–507.

111. **Vignuzzi, M., J. K. Stone, J. J. Arnold, C. E. Cameron, and R. Andino.** 2006. Quasispecies diversity determines pathogenesis through cooperative interactions in a viral population. *Nature* **439:**344–348.

112. **Wenner, H. A., P. Kamitsuka, M. Lenahan, and I. Archetti.** 1960. The pathogenesis of poliomyelitis. Sites of multiplication of poliovirus in cynomolgus monkeys after alimentary infection. *Arch. Gesamte Virusforsch.* **9:**537–558.

113. **Wessely, R., K. Klingel, K. U. Knowlton, and R. Kandolf.** 2001. Cardioselective infection with coxsackievirus B3 requires intact type I interferon signaling: implications for mortality and early viral replication. *Circulation* **103:**756–761.

114. **Westrop, G. D., K. A. Wareham, D. M. Evans, G. Dunn, P. D. Minor, D. I. Magrath, F. Taffs, S. Marsden, M. A. Skinner, G. C. Schild, et al.** 1989. Genetic basis of attenuation of the Sabin type 3 oral poliovirus vaccine. *J. Virol.* **63:**1338–1344.

115. **Yanagiya, A., S. Ohka, N. Hashida, M. Okamura, C. Taya, N. Kamoshita, K. Iwasaki, Y. Sasaki, H. Yonekawa, and A. Nomoto.** 2003. Tissue-specific replicating capacity of a chimeric poliovirus that carries the internal ribosome entry site of hepatitis C virus in a new mouse model transgenic for the human poliovirus receptor. *J. Virol.* **77:**10479–10487.

116. **Yang, W. X., T. Terasaki, K. Shiroki, S. Ohka, J. Aoki, S. Tanabe, T. Nomura, E. Terada, Y. Sugiyama, and A. Nomoto.** 1997. Efficient delivery of circulating poliovirus to the central nervous system independently of poliovirus receptor. *Virology* **229:**421–428.

117. **Yoshikawa, T., T. Iwasaki, M. Ida-Hosonuma, M. Yoneyama, T. Fujita, H. Horie, M. Miyazawa, S. Abe, B. Simizu, and S. Koike.** 2006. Role of the alpha/beta interferon response in the acquisition of susceptibility to poliovirus by kidney cells in culture. *J. Virol.* **80:**4313–4325.

118. **Zhang, S., and V. R. Racaniello.** 1997. Expression of the poliovirus receptor in intestinal epithelial cells is not sufficient to permit poliovirus replication in the mouse gut. *J. Virol.* **71:** 4915–4920.

JOURNAL OF VIROLOGY, June 2010, p. 5947–5957
0022-538X/10/$12.00 doi:10.1128/JVI.02575-09

Vol. 84, No. 12

2A Protease Is Not a Prerequisite for Poliovirus Replication▽†

Hiroko Igarashi,[1] Yasuko Yoshino,[1] Miwako Miyazawa,[2] Hitoshi Horie,[2,3] Seii Ohka,[1]* and Akio Nomoto[1]#

Department of Microbiology, Graduate School of Medicine, The University of Tokyo, 7-3-1 Hongo, Bunkyo-ku, Tokyo 113-0033, Japan[1]; Japan Poliomyelitis Research Institute, Tokyo, Japan[2]; and Department of Microbiology, Faculty of Pharmaceutical Science, Ohu University, Fukushima, Japan[3]

Received 9 December 2009/Accepted 5 April 2010

Poliovirus (PV) $2A^{pro}$ has been considered important for PV replication and is known to be toxic to host cells. A $2A^{pro}$-deficient PV would potentially be less toxic and ideal as a vector. To examine whether $2A^{pro}$ is needed to form progeny virus, a full-length cDNA of dicistronic (*dc*) PV with (pOME) or without (pOMEΔ2A) $2A^{pro}$ was constructed in the strain PV1(M)OM. RNAs of both pOME and pOMEΔ2A were capable of forming progeny viruses, called OME and OMEΔ2A, respectively. In their ability to induce a cytopathic effect (CPE), the strains ranked as OMEΔ2A < OME ≒ PV1(M)OM. These results suggest that $2A^{pro}$ is not essential for full-length *dc* PV to form progeny virus and that it contributes to the efficient viral replication and/or induction of a CPE. To clarify whether $2A^{pro}$ is essential for P1-null (lacking the entire coding sequence for capsid proteins) PV, the RNA replication activity of P1-null PV (pOMΔP1) or P1-null PV without $2A^{pro}$ (pOMΔP1Δ2A) or without both $2A^{pro}$ and 2B (pOMΔP1Δ2AΔ2B) was examined. The RNAs of pOMΔP1 and pOMΔP1Δ2A could replicate and form progeny viruses under a *trans* supply of P1 protein, whereas the RNA of pOMΔP1Δ2AΔ2B could not. These results suggest that $2A^{pro}$ is not needed for the replication of P1-null PV, although it is important for PV RNA replication and inducing a CPE. To know whether a $2A^{pro}$-deficient PV can be used as a vector, a P1-null PV containing the enhanced green fluorescent protein (EGFP) coding sequence with or without $2A^{pro}$ was examined. It expressed fluorescent protein. This result suggests that $2A^{pro}$-deficient PV can express foreign genes.

Poliomyelitis is an acute disease of the central nervous system caused by the poliovirus (PV), a human enterovirus that belongs to the *Picornaviridae* family. Humans are the only natural hosts of PV. In humans, an infection is initiated by oral ingestion of the virus followed by multiplication in the alimentary mucosa (7, 38), from where the virus spreads through the bloodstream. Viremia is considered essential for leading to paralytic poliomyelitis in humans.

PV is a nonenveloped particle that consists of a positive single-stranded RNA genome and 60 copies each of four capsid proteins and occurs in three serologically distinct types, type 1, type 2, and type 3. The genome, composed of approximately 7,500 nucleotides (nt), is polyadenylylated and covalently linked at the 5′ end to a small protein, VPg (31, 40, 44). The RNA alone is infectious; cells transfected with the RNA produce infectious progeny virions. The polyprotein is cotranslationally cleaved by virus-specific proteinases to form viral capsid proteins (VP0, VP1, and VP3) and noncapsid proteins (2A, 2B, 2C, 3A, 3B, 3C, and 3D). VP0 is further cleaved into VP2 and VP4 during the formation of virions. $2A^{pro}$, $3C^{pro}$, and $3CD^{pro}$ are viral proteinases involved in processing specific to PV polyproteins (26). The translation of the viral mRNA is controlled by an internal ribosomal entry site (IRES), a 400-nt RNA segment of the viral genome that precedes the open reading frame (ORF) (33, 34). An IRES element with a similar function exists in the genomic RNA of the encephalomyocarditis virus (EMCV) (19, 20). Molla et al. (29) inserted the type 2 EMCV IRES element into the ORF of PV (at the P1*P2 junction), thereby generating a virus carrying a dicistronic (*dc*) RNA genome. In this *dc* virus, viral proteins are produced by proteolytic processing of two distinct polyproteins, P1 and P2-P3, specifying the capsid proteins and the nonstructural proteins, respectively.

PV defective interfering particles (DIs) have been isolated from laboratory-propagated viral populations (12, 13, 21, 28) and from manipulated cloned infectious cDNAs (16) and, in all cases, retain translational as well as replication competence (28, 32). It has been reported that foreign gene sequences could be substituted into the PV P1 region without affecting the replication of the RNA (4, 37) as long as the translational reading frame was maintained (16). Since the replicons do not encode capsid proteins, they were encapsidated when transfected into cells previously infected with a recombinant vaccinia virus (VV-P1) which expresses the PV capsid precursor, P1 (36). Serial passage of these replicons in the presence of VV-P1 resulted in increasing titers of encapsidated replicons, allowing the generation of stocks of the recombinant PV vectors (36).

In addition to cleaving viral polyproteins, $2A^{pro}$ is known to cleave several cellular proteins. Cleavage of the eukaryotic translation initiation factor eIF4G by $2A^{pro}$ inhibits the cap-dependent translation of cellular mRNA without affecting the translation of viral RNA (15, 24). Independent of the shutoff of

* Corresponding author. Present address: Cancer Stem Cell Project, National Cancer Center Research Institute, 5-1-1 Tsukiji, Chuo-ku, Tokyo, 104-0045, Japan. Phone: 81-3-3547-5201, ext. 4701. Fax: 81-3-3547-5123. E-mail: sohka@ncc.go.jp.

Present address: Institute of Microbial Chemistry, Gotanda, 3-14-23 Kamiosaki, Shinagawa-ku, Tokyo 141-0021, Japan.

▽ Published ahead of print on 14 April 2010.

† The authors have paid a fee to allow immediate free access to this article.

host protein synthesis, $2A^{pro}$ also stimulated the translation of PV RNA (17). The stimulation of translation was later shown to be mediated, at least in part, by the C-terminal cleavage product of eIF4G that is generated by $2A^{pro}$ (8, 18, 45). Therefore, $2A^{pro}$ enhances viral protein synthesis in infected cells both by inhibiting host cell protein synthesis and by stimulating the translation of viral RNA. Several genetic studies suggest $2A^{pro}$ to also have an essential role in PV RNA replication. The replication of a subgenomic RNA replicon which contained a deletion mutation in $2A^{pro}$ was severely inhibited in transfected cells (14). Interestingly, the replication of this RNA could be rescued in *trans* when $2A^{pro}$ was provided by a wild-type helper RNA (14). In addition, studies using a *dc* PV RNA, where the *cis* cleavage function of $2A^{pro}$ was not required to cleave the viral polyprotein, suggested that $2A^{pro}$ activity was essential for efficient viral RNA replication (30). The C-terminal region of $2A^{pro}$ has also been implicated in viral RNA replication (27). $2A^{pro}$ also targets nuclear factors, including several transcription factors (42) and a structural component of small nuclear ribonucleoproteins (snRNPs), gemin-3, which is implicated in the removal of eukaryotic introns mediated by the spliceosome machinery (3). PV $2A^{pro}$ induces alterations in the nuclear pore complex, which inhibits the nuclear export of U snRNA, rRNA, and mRNA but not tRNA. The inhibition of trafficking of *de novo*-synthesized mRNAs occurs early after $2A^{pro}$ expression, suggesting that this protease could prevent host responses to viral infections (11).

PV induces an apoptotic response when its growth is markedly suppressed, for example, in the presence of guanidine hydrochloride. A temperature-sensitive (*ts*) mutant of PV also had suppressed viral growth and induced an apoptotic response. In contrast, a productive infection in these apoptotic cells was accompanied by a canonical necrotic cytopathic effect (CPE) (1, 2, 41). The viral infection triggers an apoptotic pathway involving the consecutive activation of caspase-9 and caspase-3. The productive viral infection suppresses the implementation of this apoptotic program, at least in part, by aberrant processing and degradation of procaspase-9 (6).

Here, we show that a $2A^{pro}$-deficient full-length *dc* PV is replication competent, although the efficiency of its replication is decreased. Moreover, a $2A^{pro}$-deficient P1-null (lacking the entire coding sequence for the capsid proteins) PV with or without enhanced green fluorescent protein (EGFP) can also produce progeny virions under a *trans* supply of P1 protein. Therefore, $2A^{pro}$ is not needed for the replication of PV with or without the P1 coding region in the viral genome, although $2A^{pro}$ plays important roles in PV RNA replication and inducing a CPE.

MATERIALS AND METHODS

Cells, viruses, and antibodies. Monolayers of HeLa and African green monkey kidney (AGMK) cells were grown in Dulbecco's modified Eagle's medium (DMEM) (Invitrogen) supplemented with 5% newborn calf serum (NCS; Mitsubishi Kasei), 0.11% $NaHCO_3$ (Wako Pure Chemical Industries Ltd.), and 0.1 mg/ml kanamycin sulfate (Meiji Seika Kaisha, Ltd.) at 37°C under 5% CO_2 and used for the preparation of viruses, transfection with infectious cDNA clones, and plaque assays.

The virulent type 1 PV strain Mahoney [PV1(M)OM], derived from an infectious cDNA clone, pOM1 (39), and the type 3 PV strain Leon were employed in this study. The viruses recovered from the cells transfected with the RNAs of pOMΔ0.8, pOMΔ1.8, pOMΔP1, pOMΔP1Δ2A, pOM-EGFPΔP1, pOM-EGFPΔP1Δ2A, pOME, and pOMEΔ2A were designated OMΔ0.8, OMΔ1.8, OMΔP1, OMΔP1Δ2A, OM-EGFPΔP1, OM-EGFPΔP1Δ2A, OME, and OMEΔ2A, respectively. For providing the PV P1 capsid precursor for P1-defective genomes, a recombinant vaccinia virus (VV-P1) was used (5).

Filtrated ascites fluid of an anti-Mahoney mouse monoclonal antibody (7m008) and an anti-Leon mouse monoclonal antibody (Thai p34-120) were used for the neutralizing assay.

Construction of recombinant cDNAs. pOMΔ0.8 was constructed with a deletion of 816 nucleotides in pOM1 from nucleotide (nt) 1663 to nt 2478 (Fig. 1). Similarly, pOMΔ1.8 had a 1,782-nucleotide deletion in pOM1 from nt 1175 to nt 2956, pOMΔP1 had a 2,628-nucleotide deletion in pOM1 from nt 746 to nt 3373, pOMΔP1Δ2A had a 3,072-nucleotide deletion in pOM1 from nt 746 to nt 3817, and pOMΔP1Δ2AΔ2B had a 3,367-nucleotide deletion in pOM1 from nt 746 to nt 4112. All these plasmids except pOMΔ1.8 were constructed by PCR using KOD Plus DNA polymerase (Toyobo). pOMΔ1.8 was constructed from pOM1 digested by NruI (nt 1172) and SnaBI (nt 2954) and self-ligated.

pOM-EGFPΔP1 was constructed by PCR, subcloning into pBluescript II KS(+), and recombination. Briefly, the fragment from nt 1 to nt 735 of pOM1 which had an XhoI restriction site downstream of nt 735 was digested by KpnI and XhoI and inserted into the equivalent sites of pBluescript II KS(+). This plasmid was designated pBS(1). A fragment amplified from pEGFP-N1 (Clontech) by PCR using a sense primer (MunI>EGFP; 5′-CCCAATTGTATCATA ATGGTGAGCAAGGCG-3′) and an anti-sense primer (EGFP<SmaI; 5′-TCC CCCGGGCTTGTACAGCTCGT-3′) was digested by MunI and SmaI and inserted into the equivalent sites of pBS(1). This plasmid was designated pBS(2). A fragment from nt 3365 to nt 4252 of pOM1 which had a SmaI restriction site just upstream of nt 3365 was digested by SmaI and SpeI (nt 3982 of pOM1) and inserted into the equivalent sites of pBS(2). This plasmid was designated pBS(3). pBS(3) was digested by KpnI and inserted into the equivalent sites of pOM1 (nt 66 and nt 3660). pOM-EGFPΔP1Δ2A was similarly constructed except for the final recombination sites (KpnI [nt 66 of pOM1] and SpeI [nt 3982 of pOM1]).

pOME was constructed by PCR from pOM1 and a plasmid which contains the IRES of EMCV. A fragment containing the PV IRES and P1 coding region with a termination codon which had an EcoRI restriction site just downstream of the termination codon was digested by Bpu1102I (nt 285 of pOM1) and EcoRI (fragment 1). The other fragment contained an EMCV IRES-related region (nt 214 to nt 852 of EMCV cDNA) which had an EcoRI restriction site just upstream of nt 214 of EMCV cDNA and a SmaI restriction site downstream of nt 852 of EMCV cDNA. The sequence of the junction was 5′-(EMCV IRES)-ATG GCC ACA ACC ATG GAA CCC GGG-(SmaI restriction site)-3′. This fragment was digested by EcoRI and SmaI (fragment 2), and fragment 1 and fragment 2 were inserted between the Bpu1102I and SmaI sites of pBluescript II SK(+). This plasmid was designated pBS(4). pBS(4) was digested by Bpu1102I and SmaI (fragment 3). A fragment containing the PV P2-P3 coding region which had a SmaI restriction site just upstream of the sequence required for PV $2A^{pro}$ digestion between PV P1 and $2A^{pro}$ was digested by SmaI and BglII (nt 5601 of pOM1) (fragment 4). The sequence of the junction between the SmaI restriction site and the 2A coding sequence was 5′-(SmaI restriction site) ACC TAC ($2A^{pro}$ coding sequence)-3′. Fragments 3 and 4 were inserted between the Bpu1102I and BglII sites of pOM1, and the final plasmid was designated pOME. pOMEΔ2A was constructed similarly to pOME. The sequence of the junction between the SmaI restriction site and 2B coding sequence was 5′-(SmaI recognition site) GAA GCC ATG GAA CAA (2B coding sequence)-3′.

Nucleotide sequences derived from PCR fragments were analyzed using a BigDye terminator cycle sequencing kit (version 3 or 3.1) (Applied Biosystems) with an ABI Prism 310 genetic analyzer (Applied Biosystems) or ABI Prism 3100 Avant genetic analyzer (Applied Biosystems).

RNA transfection. RNA transcripts were synthesized from PvuI-linearized cDNAs using an AmpliScribe T7 high-yield transcription kit (Epicentre Biotechnologies) and digested with RNase-free DNase I. AGMK cells on a 6-cm dish (Falcon) were transfected with 1 to 3 μg of RNA by a DEAE-dextran method (16). The cultures were harvested at 42 h [for PV1(M)OM and OME] or 75 h (for OMEΔ2A) after the transfection. OMEΔ2A was serially passaged through AGMK cells two times.

Reverse transcription (RT)-PCR. RNA was extracted from PV1(M)OM, OME, OMEΔ2A, OM-EGFPΔP1, and OM-EGFPΔP1Δ2A with chloroform containing phenol and isoamyl alcohol and reverse transcribed with Superscript II transcriptase (Invitrogen) using an anti-sense primer (PV5699<5719 or PV4784<4805). PCR was then performed with KOD Plus (Toyobo) using a sense primer [PV(M)2955>2923] and an anti-sense primer [PV(M)4232<4252] for PV1(M)OM, OME, and OMEΔ2A or using a sense primer (PV577>597) and an anti-sense primer (PV4512<4431) for OM-EGFPΔP1 and OM-EGFPΔP1Δ2A. The PCR products were analyzed by agarose gel electrophoresis.

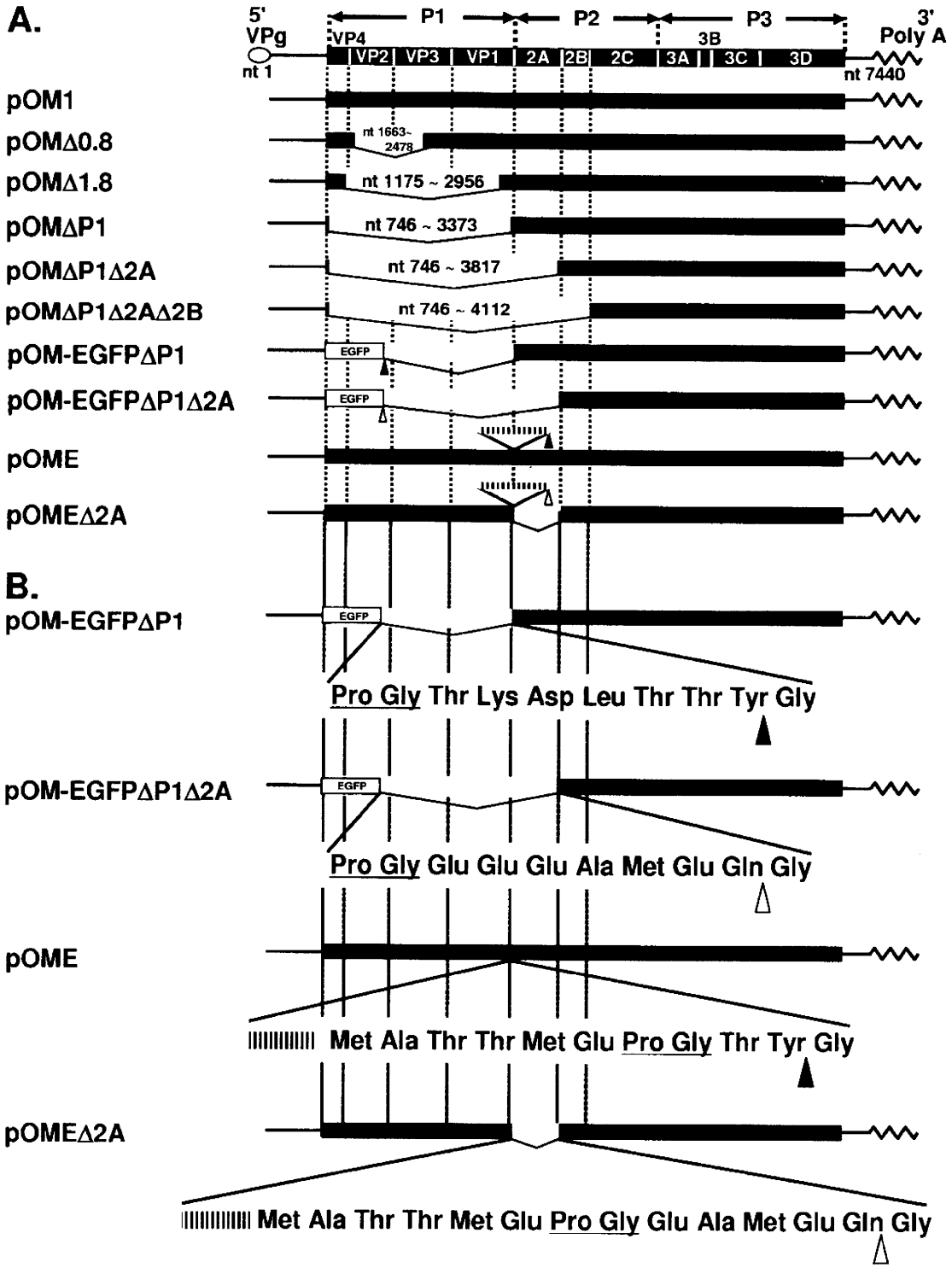

FIG. 1. PV genomic constructions. (A) Construction of PV and recombinant PVs. (B) Junctional amino acid sequences of pOM-EGFPΔP1, pOM-EGFPΔP1Δ2A, pOME, and pOMEΔ2A. The nucleic acid sequence (CCCGGG) recognized by SmaI, corresponding to the amino acid sequence Pro Gly, is shown by underlines. The inserted EMCV IRES are shown by the striped horizontal bars. Closed triangles indicate the sites of cleavage by $2A^{pro}$, and open triangles indicate the sites of cleavage by $3C^{pro}$ or $3CD^{pro}$. Nucleotide numbers of the deleted fragments are shown at the deletion positions.

For sequencing of the products, DNA was extracted from the gels using GenElute Minus ethidium bromide spin columns (Sigma).

Slot blot analysis. Monolayers of HeLa cells (4.4×10^5 cells/well) in 6-well plates were transfected with the *in vitro*-synthesized RNA from each plasmid by the DEAE-dextran method or infected with the viruses. At the time points indicated below, cytoplasmic RNA was extracted from the transfected cells using Isogen (Nippon Gene Co., Ltd.) dissolved in 40 μl of H_2O. One-fourth was mixed with 30 μl of denaturation buffer (66% [vol/vol] formamide and 7.8%

[vol/vol] formaldehyde) in 3-(*N*-morpholino)propanesulfonic acid (MOPS) buffer (26 mM MOPS [pH 7.0], 6.5 mM sodium acetate, and 1.3 mM EDTA) and denatured at 65°C for 5 min, followed by chilling on ice. An equal volume of 20× SSC (333 mM NaCl and 333 mM sodium citrate tribasic dehydrate) was added. In each slot of a slot blotting apparatus (Bio-Dot SF; Bio-Rad Laboratories, Inc.), 10 μl of RNA solution was applied, and the RNA was immobilized on a nylon filter (Hybond-N; GE Healthcare UK Ltd.) and cross-linked by a UV cross-linker (UV Stratalinker1800; Stratagene). The filters were hybridized to a labeled cDNA corresponding to nt 1 to nt 742 of the viral RNA (43) or to exon 7 of glycerol-3-phosphate dehydrogenase (GAPDH) mRNA using AlkPhos Direct (GE Healthcare UK Ltd.) according to the manufacturer's instructions. The probes were detected by chemiluminescence using CDP-Star (GE Healthcare UK Ltd.).

Encapsidation of PV replicons, serial passaging, and purification. The encapsidation and serial passaging of PV replicons using VV-P1 have been described previously (5), and basically the same method was adopted here. Briefly, HeLa S3 cells were infected with 5 PFU of VV-P1, which expresses the PV capsid precursor protein P1, per cell. At 2 h postinfection, the cells were transfected by the DEAE-dextran method with *in vitro*-transcribed RNA. The cultures were harvested at 24 h posttransfection by three successive freeze-thaws, sonicated, and clarified by low-speed centrifugation at 14,000 × *g* for 20 min. For serial passage of the encapsidated replicons and generation of virus stocks, HeLa S3 cells were first infected with 10 to 20 PFU of VV-P1 per cell. At 2 h postinfection, the cells were infected with passage 1 encapsidated replicons. The cultures were harvested at 16 h after PV infection by three successive freeze-thaws, sonicated, and clarified by low-speed centrifugation at 14,000 × *g* for 20 min. The supernatant was then stored at −80°C or used immediately for additional passages by the same procedure.

For purifying the P1-null PV particles, the supernatant was lysed with 1% sodium dodecyl sulfate and centrifuged in a Beckman type 45 rotor at 35,000 rpm for 2.5 h. The supernatant was discarded, and the pellet was washed under the same conditions in 0.1 M phosphate buffer (pH 7.35) for an additional 2.5 h. The pellet was then resuspended in serum-free DMEM, filtrated, and stored at −80°C.

Titration of viruses. The numbers of PFU in AGMK cells were determined by the plaque assay, and the numbers of infectious units (IU) were determined by counting fluorescence-positive cells. Units of viral RNA (U) were adopted for the infection with P1-null viruses. For the measurement of PFU, AGMK cells on 6-cm dishes were inoculated with the viral suspension and then incubated at 37°C for 2 to 5 days for the observation of plaques. To measure the units of viral RNA of OMΔ0.8, OMΔ1.8, OMΔP1, and OMΔP1Δ2A, viral RNA was extracted from the suspensions with chloroform containing phenol and isoamyl alcohol. The units were measured using a LightCycler system (Roche Diagnostics) according to the manufacturer's instructions. As 1.1×10^8 U/ml was equivalent to 2.1×10^9 PFU/ml for PV1(M)OM, we adopted 5.2×10^1 U/cell, which was supposed to be equivalent to 1,000 PFU/cell (multiplicity of infection [MOI] of 1,000) of PV1(M)OM for the infection with OMΔ0.8, OMΔ1.8, OMΔP1, and OMΔP1Δ2A. For the measurement of IU of OM-EGFPΔP1 and OM-EGFPΔP1Δ2A, fluorescence-positive cells were counted under an inverted fluorescence microscope (DM6000B; Leica Microsystems) at 24 h postinfection in HeLa cells. The amount of virus leading to one fluorescence-positive cell was defined as 1 IU. Comparing the units of RNA with the infectious units of fluorescence-positive cells, 5.3×10^9 U/ml was equivalent to 7.1×10^9 IU/ml for an OM-EGFPΔP1 stock and 4.2×10^9 U/ml was equivalent to 1.1×10^9 IU/ml for an OM-EGFPΔP1Δ2A stock. Based on the data, we considered that the units of RNA were not significantly different from the infectious units for OM-EGFPΔP1 and OM-EGFPΔP1Δ2A.

Observation of CPE. HeLa S3 cells in 16-well Lab-Tek chamber slides (Nalge Nunc International K.K.) were infected with PVs. Eight, 18, or 24 h after the incubation with PVs at 37°C, the cells were observed under an inverted microscope.

Neutralization assay. The viral suspension (50 μl) was mixed with filtrated ascites fluid (50 μl) containing the antibody and incubated at 37°C for 1 h. The virus-antibody mixture was overlaid on HeLa S3 cells in 16-well chamber slides and incubated at room temperature for 20 min and then at 37°C for 30 min. The mixture was then replaced with DMEM supplemented with 5% NCS. The cells were observed 18 h after the incubation at 37°C under an inverted microscope.

TUNEL assay. A direct terminal deoxynucleotidyltransferase mediated dUTP-biotin nick end labeling (TUNEL) assay was performed using an *in situ* cell death detection kit (Roche Diagnostics), and cells were observed under a confocal laser scanning microscope (LSM510; Carl Zeiss MicroImaging Co. Ltd.). Actinomycin D (10 μg/ml) was added for an apoptosis positive control.

RESULTS

$2A^{pro}$ is not required for full-length *dc* PV to form progeny virus. $2A^{pro}$ is known to be cytotoxic, and a $2A^{pro}$-deficient PV vector might be desirable. To examine whether $2A^{pro}$ is needed to form progeny virus, cDNAs of the full-length *dc* pOME and pOMEΔ2A with the backbone of the PV type 1 Mahoney strain (pOM1) (Fig. 1A and B) were constructed and the ability to form progeny viruses was examined. HeLa cells were transfected with the RNA of pOM1, pOME, and pOMEΔ2A and examined for a CPE. RNA derived from pOM1, pOME, and pOMEΔ2A was not degraded as assessed by gel electrophoresis (data not shown). All these RNAs induced a CPE that led to cell death, whereas no CPE was observed in the mock-transfected cells (data not shown). The supernatants also induced a CPE in HeLa cells. These results show that pOM1, pOME, and pOMEΔ2A can form progeny viruses, called PV1(M)OM, OME, and OMEΔ2A, respectively. This suggests that $2A^{pro}$ is not essential to form progeny virus for full-length *dc* PV.

To confirm that the OME and OMEΔ2A suspensions do not contain IRES deletion revertants, the sizes of the fragments encompassing VP1 and 2B were examined by PCR (data not shown). The PV1(M)OM, OME, and OMEΔ2A suspensions produced appropriate fragments, that is, 1.3-kb, 1.9-kb, and 1.5-kb fragments, respectively. The sequences of the PCR fragments were analyzed, and they were not mutated (data not shown). These results mean that IRES deletion revertants were not detected in the OME and OMEΔ2A suspensions under the experimental conditions and that it is highly probable that these suspensions do not contain IRES deletion revertants. This suggests that OME and OMEΔ2A can proliferate by themselves.

To ascertain that the CPE was actually induced by PV, a neutralization assay was performed using a monoclonal antibody for the virulent type 1 Mahoney strain (7m008) and a monoclonal antibody for the virulent type 3 Leon strain (Thai p34-120). HeLa cells were infected with PV1(M)OM, OME, OMEΔ2A, or Leon at an MOI of 10 in the presence or absence of 7m008 or Thai p34-120 and examined for a CPE (Fig. 2). In the absence of the antibodies, all the strains induced a CPE. In the presence of 7m008, only Leon caused a CPE. In contrast, in the presence of Thai p34-120, all the strains except Leon had a CPE. These results suggest that PV1(M)OM, OME, and OMEΔ2A are type 1 strains, and the CPE was induced by PV.

To define the characteristics of the viral strains, a plaque assay was performed using AGMK cells (Fig. 3). PV1(M)OM produced large plaques, OME moderate-sized plaques, and OMEΔ2A the smallest plaques. The extremely small plaques of OMEΔ2A may relate to its slow replication rate.

To compare these strains further, HeLa cells were infected at an MOI of 10 and cell morphology was observed 8 or 24 h after the infection (Fig. 4). All the viruses had a CPE (Fig. 4A). No CPE was observed in the mock-infected cells. To quantify the rate of CPE-expressing cells, the percentages of round-shaped cells, detached cells, and cells with membrane blebbing among all cells were analyzed, and the kinetics are shown in Fig. 4B. OMEΔ2A had a lesser CPE than did OME or PV1(M)OM. OME exhibited a similar level of CPE to PV1(M)OM, although OME had slightly slower kinetics than

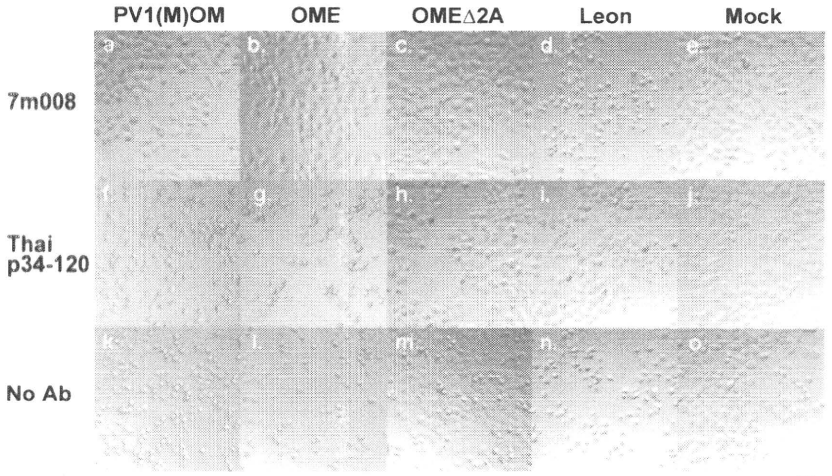

FIG. 2. Neutralization assay of PV1(M)OM, OME, OMEΔ2A, and Leon with anti-PV type 1 or type 2 monoclonal antibody. HeLa cells were mock infected (e, j, and o) or infected with PV1(M)OM (a, f, and k), OME (b, g, and l), OMEΔ2A (c, h, and m), or Leon (d, i, and n) in the absence (k to o) or presence of an anti-PV type 1 Mahoney monoclonal antibody (7m008, a to e) or anti-PV type 2 Leon monoclonal antibody (Thai p34-120, f to j). Eighteen hours after the infection, the CPE was observed under a microscope. Bar, 50 μm.

PV1(M)OM. The results were reproducible. These results suggest that in speed of viral replication and/or the ability to induce CPE, the strains rank as OMEΔ2A < OME ≒ PV1(M)OM. They also suggest that $2A^{pro}$ contributes to efficient viral replication and/or the induction of a CPE. When the cells were infected at a higher MOI (MOI of 50), the kinetics were essentially unchanged (data not shown). This result suggests that an MOI of 10 was high enough to assess the kinetics of CPE expression. Only OMEΔ2A induced morphological changes typical of apoptosis, namely, cell membrane blebbing, in a significant proportion of cells (Fig.4Ac, Ae, and 4Cs). This result indicates that OMEΔ2A may induce apoptosis.

$2A^{pro}$-deficient full-length *dc* PV induces apoptosis. To confirm that OMEΔ2A induces apoptosis, a direct TUNEL assay was performed in cells infected with or without PV1(M)OM or OMEΔ2A or treated with actinomycin D, which induces apoptosis (Fig. 5). Uninfected samples and PV1(M)OM-infected samples contained few fluorescence-positive cells. On the other hand, actinomycin D-treated samples and OMEΔ2A-infected samples included many fluorescence-positive cells. These results suggest that OMEΔ2A induces apoptosis. This raises the possibility that $2A^{pro}$ is important to prevent typical apoptosis in PV-infected cells.

P1-null PV RNA deficient in the $2A^{pro}$ coding region can replicate in cells. It has been reported that the PV P1 coding region is not required for RNA replication and the formation of progeny virus in P1-expressing cells (4, 37). To further define which parts of the PV genome are necessary for RNA replication, deletion mutants were prepared (Fig. 1A) and RNA replication activity was examined by slot blotting (Fig. 6A). RNAs derived from pOM1, pOMΔ0.8, pOMΔ1.8, pOMΔP1, pOMΔP1Δ2A, and pOMΔP1Δ2AΔ2B were not degraded as assessed by gel electrophoresis (data not shown). The RNAs were introduced into HeLa cells, and the cells were collected 2 and 8 h after the transfection. Cell lysates were used for slot blotting. When a probe for PV IRES RNA was used, all the RNAs except for pOMΔP1Δ2AΔ2B RNA were increased at 8 h compared to the levels at 2 h after the transfection. The amounts of GAPDH RNA hardly changed up to 8 h after the transfection. The results were reproducible. These results suggest that the $2A^{pro}$ coding region is not needed for the RNA replication of P1-null PV and that 2B is necessary for the PV replicon activity.

The $2A^{pro}$ coding region is not required for P1-null PV to form progeny virus in P1-expressing cells. Next, the ability to form progeny virus was examined. The RNAs of pOM1,

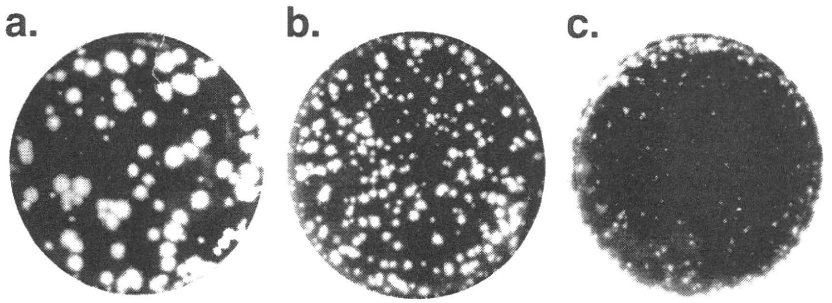

FIG. 3. Plaque phenotypes of PV1(M)OM, OME, and OMEΔ2A. AGMK cells were infected with PV1(M)OM (a), OME (b), and OMEΔ2A (c). The cells were fixed 2 days after the infection with PV1(M)OM, and OME and 4 days after the infection with OMEΔ2A.

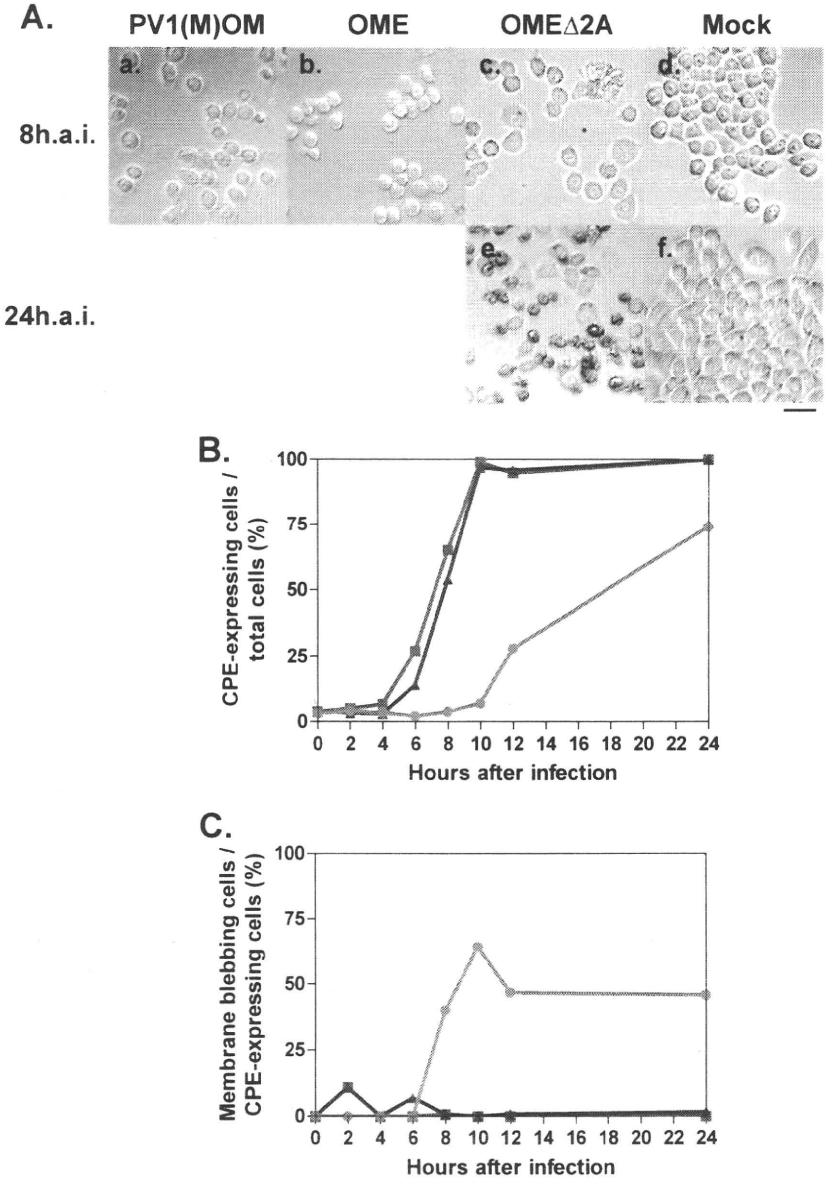

FIG. 4. CPE in cells infected with or without PV1(M)OM, OME, and OMEΔ2A. (A) HeLa cells were mock infected (d and f) or infected with PV1(M)OM (a), OME (b), or OMEΔ2A (c and e) at an MOI of 10. Eight (a to d) or 24 h (e and f) after the infection (h.a.i.), morphological changes were observed under a microscope. Bar, 50 μm. (B) Percentages of CPE expression among all cells. (C) Rates of membrane blebbing among CPE-expressing cells. Average rates in two to three microscopic fields in one experiment were plotted. The rates were examined 0, 2, 4, 6, 8, 10, 12, and 24 h after the infection. Blue lines with squares indicate results for PV1(M)OM, pink lines with triangles indicate results for OME, and orange lines with circles indicate results for OMEΔ2A.

pOMΔ0.8, pOMΔ1.8, pOMΔP1, pOMΔP1Δ2A, and pOMΔP1Δ2AΔ2B were introduced into P1-expressing cells, and the supernatant was recovered after freezing and thawing. HeLa cells were covered with medium containing the supernatants and examined for a CPE 24 h later (data not shown). All the supernatants except those of pOMΔP1Δ2AΔ2B RNA and mock transfectants had a CPE. These results suggest that the RNAs of pOMΔ0.8, pOMΔ1.8, pOMΔP1, and pOMΔP1Δ2A can form progeny viruses, OMΔ0.8, OMΔ1.8, OMΔP1, and OMΔP1Δ2A, respectively, whereas the pOMΔP1Δ2AΔ2B RNA cannot. The quality and sizes of the viral RNA genomes were confirmed by agarose gel electrophoresis (data not shown). To adjust the titers among these viruses, the copy numbers of the PV RNA strands in the virus-containing supernatants were examined by quantitative real-time PCR and the units of viral RNA were determined. To examine the CPE expression, HeLa cells were infected at 5.2×10^1 U/cell and examined for a CPE up to 24 h after the infection (Fig. 7), and the rates of round cells, detached cells, and cells with membrane blebbing among all cells were analyzed (Fig. 7B). Similar to the previous results, all the viruses had a CPE. P1-null PV had slower kinetics than PV1(M)OM. OMΔ0.8, OMΔ1.8, and OMΔP1 showed similar numbers of CPE-expressing cells, although the kinetics of OMΔP1 until 10 h after the infection was faster than that of other P1-null PVs.

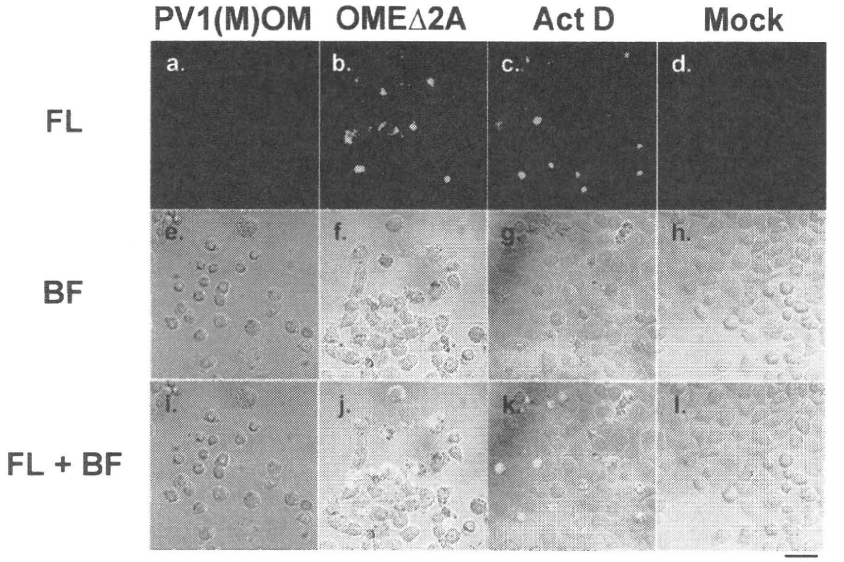

FIG. 5. Apoptosis in cells infected with OMEΔ2A, detected by the TUNEL assay. HeLa cells were mock infected (d, h, and l), infected with PV1(M)OM (a, e, and i) or OMEΔ2A (b, f, and j), or treated without (d, h, and l) or with (c, g, and k) actinomycin D (Act D). Seven hours after the infection with PV1(M)OM, 8 h after the treatment with actinomycin D, and 21 h after the infection with OMEΔ2A, the cells were TUNEL stained. TUNEL-positive cells were fluorescent. Fluorescence (FL) images are shown at the top (a to d), bright-field (BF) images are shown in the middle (e to h), and merged (FL+BF) images are shown at the bottom (i to l). Bar, 50 μm.

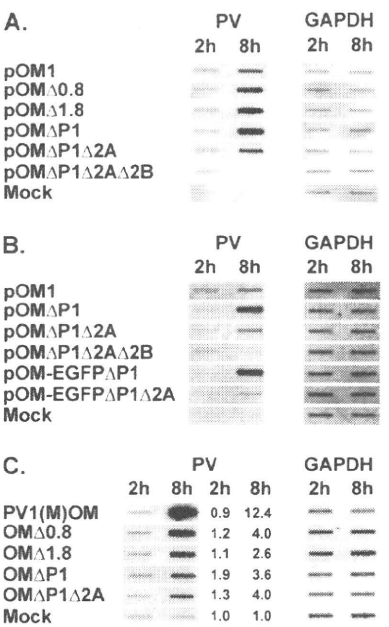

FIG. 6. Slot blot analysis of cells after transfection with or without synthesized viral RNA or after infection with or without viruses. (A) HeLa cells were transfected with or without (Mock) RNAs of pOM1, pOMΔ0.8, pOMΔ1.8, pOMΔP1, pOMΔP1Δ2A, or pOMΔP1Δ2AΔ2B, and cell lysates were collected 2 and 8 h later. The RNAs were detected with probes for the PV IRES sequence or GAPDH sequence. (B) A similar experiment was performed using the RNAs of pOM1, pOMΔP1, pOMΔP1Δ2A, pOMΔP1Δ2AΔ2B, pOM-EGFPΔP1, and pOM-EGFPΔP1Δ2A. (C) HeLa cells were infected with or without (Mock) PV1(M)OM, OMΔ0.8, OMΔ1.8, OMΔP1, or OMΔP1Δ2A, and cell lysates were collected 2 and 8 h later. The RNAs were detected with probes for the PV IRES sequence or GAPDH sequence. Relative amounts of PV RNA corrected to the amount of GAPDH RNA are shown.

OMΔP1Δ2A reproducibly had a lower rate of CPE than other P1-null PVs until 24 h after the infection. This result suggests that OMΔP1Δ2A is less able to induce a CPE or else takes longer and that $2A^{pro}$ plays an important role in inducing a CPE. OMΔP1, significantly, started to cause membrane blebbing typical of apoptosis from 2 h after the infection, and the proportion of CPE-expressing cells was relatively high at early time points (Fig. 7C). This result indicates the possibility that OMΔP1 induces apoptosis. Compared with other P1-null PVs, OMΔP1Δ2A showed at least about a two-times-higher rate of membrane blebbing among CPE-expressing cells at 24 h after infection (OMΔ0.8, 12%; OMΔ1.8, 4.7%; OMΔP1, 7.9%; and OMΔP1Δ2A, 20%) (Fig. 7C). This indicates that OMΔP1Δ2A may induce apoptosis at a relatively low efficiency.

$2A^{pro}$ coding region-deficient P1-null PV vector expresses foreign genes. Because OMΔP1Δ2A can form progeny virus, $2A^{pro}$ may not be essential for P1-null PV to express foreign genes. To examine whether OMΔP1 and OMΔP1Δ2A can express foreign genes, an EGFP coding sequence was inserted into the region of pOMΔP1 and pOMΔP1Δ2A with P1 deleted (Fig. 1A and B). The new constructs were designated pOM-EGFPΔP1 and pOM-EGFPΔP1Δ2A, respectively. RNAs derived from pOM1, pOMΔP1, pOMΔP1Δ2A, pOMΔP1Δ2AΔ2B, pOM-EGFPΔP1, and pOM-EGFPΔP1Δ2A were not degraded as assessed by gel electrophoresis (data not shown). The RNAs were introduced into HeLa cells, and the cells collected 2 and 8 h after the transfection. The cell lysate was used for slot blotting (Fig. 6B). When a probe for PV IRES RNA was used, all the RNAs except for pOMΔP1Δ2AΔ2B RNA increased at 8 h after the transfection compared to the levels at 2 h. pOM-EGFPΔP1 RNA increased more than pOM-EGFPΔP1Δ2A RNA. The amounts of GAPDH RNA hardly changed up to 8 h after the transfection. The results were reproducible. These results suggest that the $2A^{pro}$ coding region is not required for the RNA repli-

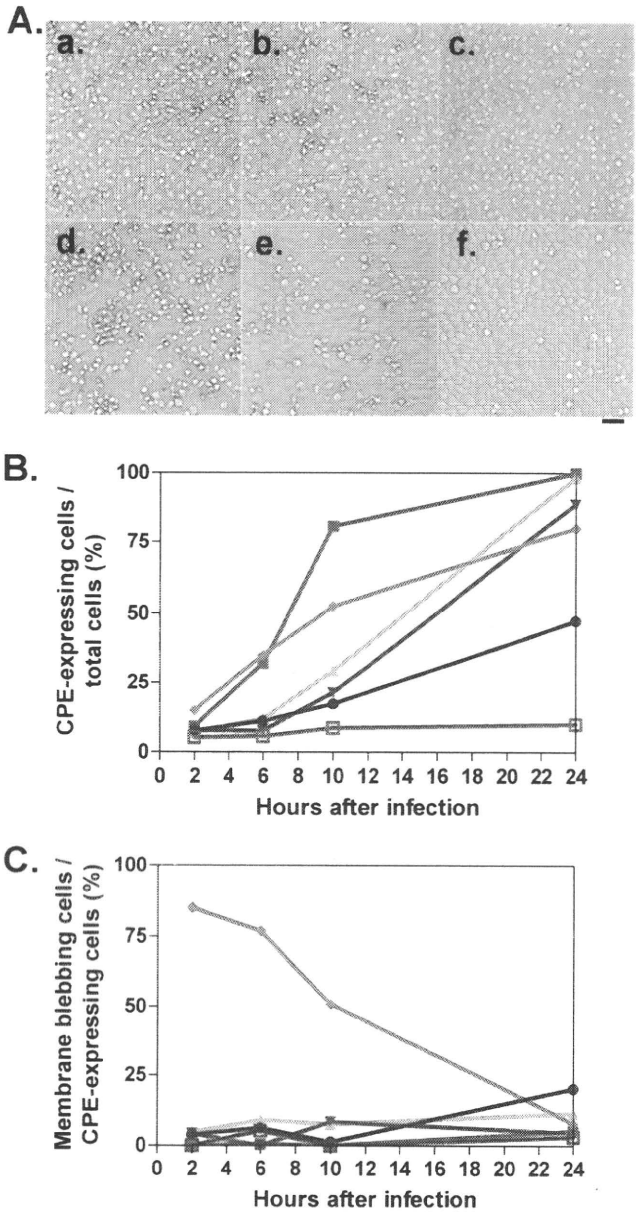

FIG. 7. CPE in the cells infected with PV1(M)OM, OMΔ0.8, OMΔ1.8, OMΔP1, and OMΔP1Δ2A. (A) HeLa cells were mock infected (f) or infected with PV1(M)OM (a), OMΔ0.8 (b), OMΔ1.8 (c), OMΔP1 (d), or OMΔP1Δ2A (e) at an MOI of 1,000, and cell morphology was observed 24 h later under a microscope. Bar, 50 μm. (B) Percentages of CPE expression among all cells. (C) Rates of membrane blebbing among CPE-expressing cells. Average rates in two to four microscopic fields in one experiment were plotted. The rates were examined at 2, 6, 10, and 24 h after the infection. Blue lines with filled squares indicate results for PV1(M)OM, green lines with triangles indicate results for OMΔ0.8, violet lines with inverted triangles indicate results for OMΔ1.8, orange lines with rhombuses indicate results for OMΔP1, pink lines with circles indicate results for OMΔP1Δ2A, and moss-green lines with open squares indicate results for mock-infected cells.

cation of P1-null PV with EGFP inserted, although deletion of the $2A^{pro}$ coding region results in a lower rate of RNA replication. When a probe for PV IRES RNA was used, the RNAs of pOMΔP1 and pOMΔP1Δ2A reproducibly increased to levels similar to the RNAs of pOM-EGFPΔP1 and pOM-EGFPΔP1Δ2A, respectively. These results suggest that the insertion of EGFP does not significantly affect PV RNA replication. Next, the RNAs of pOM-EGFPΔP1 and pOM-EGFPΔP1Δ2A were introduced into P1-expressing cells and the supernatants were recovered after freezing and thawing. The viral particles, OM-EGFPΔP1 and OM-EGFPΔP1Δ2A, respectively, proliferated in P1-expressing cells and were then purified. HeLa cells were covered with the purified virus at an MOI of 100, and the fluorescence of EGFP was observed under the fluorescence microscope 24 h after the infection (Fig. 8). Fluorescence-positive cells were observed in the OM-EGFPΔP1- and OM-EGFPΔP1Δ2A-infected samples, whereas no positive cells were observed in the mock-infected sample. These results suggest that OMΔP1 and OMΔP1Δ2A can express EGFP and that $2A^{pro}$ is not essential for P1-null PV to express EGFP.

In their ability to express EGFP 24 h after the infection, the strains ranked reproducibly as OM-EGFPΔP1Δ2A < OM-EGFPΔP1 (the average rates of fluorescence positivity among all cells in three microscopic fields in one experiment were 23% for OM-EGFPΔP1 and 9.7% for OM-EGFPΔP1Δ2A). This suggests that the defect in $2A^{pro}$ decreases the expression of EGFP and/or the speed of viral replication. OM-EGFPΔP1Δ2A had a CPE, as did OM-EGFPΔP1, but only OM-EGFPΔP1Δ2A reproducibly induced morphological changes typical of apoptosis in a significant proportion of the CPE-expressing cells (the average rates of membrane blebbing among CPE-expressing cells were 10% for OM-EGFPΔP1 and 37% for OM-EGFPΔP1Δ2A). The result implies that $2A^{pro}$ masks apoptosis in a significant proportion of cells. In the speed with which they induced a CPE, the strains reproducibly ranked as OM-EGFPΔP1 ≒ OM-EGFPΔP1Δ2A (the average rates of CPE expression among all cells were 27% for OM-EGFPΔP1 and 26% for OM-EGFPΔP1Δ2A). This suggests that $2A^{pro}$ has little or no effect on inducing a CPE. The quality and sizes of the RNA genomes of OM-EGFPΔP1 and OM-EGFPΔP1Δ2A were confirmed by Northern blotting (data not shown). The genomic stability of OM-EGFPΔP1 and OM-EGFPΔP1Δ2A was examined by general RT-PCR, but no deletion was detected even after 20 passages (data not shown). These results suggest that both OM-EGFPΔP1 and OM-EGFPΔP1Δ2A are genetically stable for at least 20 passages.

DISCUSSION

$2A^{pro}$ has been thought important for PV replication. Here, we reveal that $2A^{pro}$ is not required for PV replication and $2A^{pro}$-deficient PV with or without the capsid coding region can produce progeny viruses. This shows the possibility of realizing a vector that expresses a longer foreign gene and is less toxic.

Molla et al. reported that *dc* PV cDNA without the $2A^{pro}$ coding region (pT7PVE2B) does not produce a viable virus (30). In contrast, RNA of pOMEΔ2A, which has a structure similar to that of pT7PVE2B, resulted in productive although inefficient replication. This may be due to a difference in the junctional sequences between P1 and 2B. In the case of pT7PVE2B, 2B is translated directly from the second EMCV IRES and methionine is added to the N terminus of 2B. On the other hand, in the case of pOMEΔ2A, the additional N-termi-

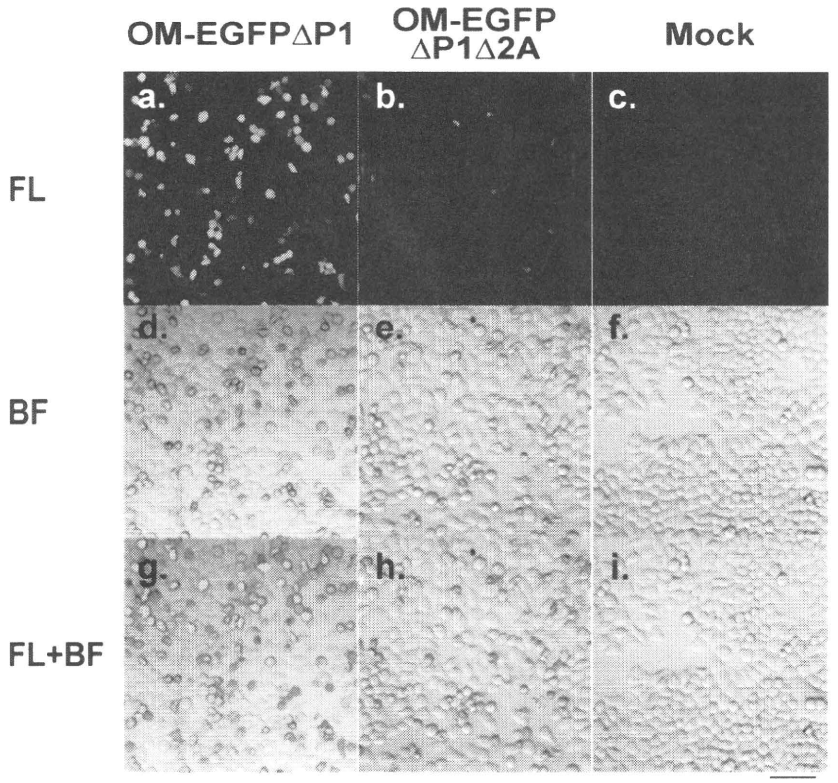

FIG. 8. P1-null PV vector with or without the $2A^{pro}$ coding region expresses EGFP. HeLa cells were mock infected (c, f, and i) or infected with OM-EGFPΔP1 (a, d, and g) or OM-EGFPΔP1Δ2A (b, e, and h) and observed 24 h later under a fluorescence microscope. Upper panels show fluorescence (FL) images (a to c), panels in the middle show bright-field (BF) images (d to f), and lower panels show merged (FL+BF) images (g to i). Bar, 100 μm.

nal sequences of 2B can be processed by $3C^{pro}$ or $3CD^{pro}$. Moreover, pT7PVE2B contains EMCV IRES up to AUG_{834}, whereas pOMEΔ2A contains it up to +18 nt downstream of AUG_{834}. Ribosomal initiation complexes attach directly to AUG_{834}, and initiation does not involve scanning (22, 35). The interaction positions for ribosomal initiation complexes are up to +17 nt downstream of AUG_{834} (23). It is possible that the difference leads to modification of the 2B activity and/or relatively low efficiency of the initiation of the second cistron translation.

OMEΔ2A caused apoptosis, whereas neither PV1(M)OM nor OME did. Our results show the possibility that OMΔP1, OMΔP1Δ2A, and OM-EGFPΔP1Δ2A induce apoptosis in a significant proportion of cells. Calandria et al. reported that independently expressed $2A^{pro}$ and $3C^{pro}$ induced apoptosis by mechanisms involving caspase activation (10). On the other hand, Burgon et al. reported that a 2A N32D mutation independently caused cells to die by apoptosis much earlier than wild-type-infected cells (9). This is consistent with the hypothesis that a wild-type function of the $2A^{pro}$ protein is to inhibit apoptosis and cause a canonical necrotic CPE late in infection, perhaps directly or indirectly leading to the aberrant cleavage of procaspase-9, and that this activity is abrogated by the 2A N32D mutation. Together with our results, it seems likely that the apoptotic cell death induced in the cells infected with 2A-deficient or P1-deficient PV occurs via caspase-dependent apoptosis and that the expression of apoptosis depends on a subtle balance of relating proteins, such as $2A^{pro}$, $3C^{pro}$, and procaspase-9, at each time point after the infection. It is highly possible that the balance of viral proteins differs depending on whether the virus is monocistronic or dicistronic. $2A^{pro}$ activity may differ fundamentally depending on whether this protein is expressed individually or in the context of the viral infection.

It has been reported that PV was replication competent upon the replacement of its P1 region with a foreign gene in P1-expressing cells (4, 37). In these cases, an insert of about 2.9 kilobases (carcinoembryonic antigen [CEA]) was the longest. DIs with a 1,212-base deletion at the longest in the P1 region have been detected (25). We revealed that PV can produce progeny viruses with the entire P1 and $2A^{pro}$ coding region deleted in P1-expressing cells. This construct lacks the longest region. We confirmed that PV can express EGFP without the P1 and $2A^{pro}$ coding regions and that the insertion of EGFP does not significantly affect viral RNA replication. Moreover, these viruses are genetically stable. These results raise the possibility that a longer foreign gene than CEA can be expressed using the PV vector.

OMΔP1Δ2A had a lesser CPE than OMΔ0.8, OMΔ1.8, OMΔP1, and PV1(M)OM at 5.2×10^1 U/cell, which was supposed to be equivalent to an MOI of 1,000 of PV1(M)OM. To correct the units of viral RNA genomes as infectious units, HeLa cells were infected with OMΔ0.8, OMΔ1.8, OMΔP1, and OMΔP1Δ2A at 5.2×10^1 U/cell or with PV1(M)OM at an MOI of 10, the cells were collected 2 and 8 h later, and cell

lysates were used for slot blotting (Fig. 6C). When a probe for PV IRES RNA was used, all the P1-null viruses had increased at almost the same rates at 8 h compared to the levels at 2 h after the infection. PV1(M)OM increased much more than P1-null viruses. These results suggest that 5.2×10^1 U/cell for P1-null viruses results in similar RNA replication activities under these conditions. The viral titers/cell might not be high enough to infect all the cells because the cells infected at 5.2×10^1 U/cell contained more RNA than those infected at 5.2 U/cell (data not shown); it is likely that the units of the RNA genomes of OMΔ0.8, OMΔ1.8, OMΔP1, and OMΔP1Δ2A were almost proportional to these RNA replication activities. Consequently, it was confirmed that OMΔP1Δ2A is less toxic or takes a longer time to have a CPE even though its RNA replication activity is similar to those of OMΔ0.8, OMΔ1.8, and OMΔP1.

Regarding the slot blot analysis of the cells transfected with synthesized viral RNA, the RNAs of pOMΔP1Δ2A and pOM-EGFPΔP1Δ2A showed less RNA replication activity than those of pOMΔP1 and pOM-EGFPΔP1, respectively (Fig. 6B). It seems likely that the defect in $2A^{pro}$ suppresses the RNA replication activity. In terms of the relevant effect of $2A^{pro}$, viral replication speed, and/or the ability to induce a CPE, the ranking was OMEΔ2A < OME and OMΔP1Δ2A < OMΔP1, whereas OM-EGFPΔP1 ≒ OM-EGFPΔP1Δ2A. In the ability to express EGFP, the ranking was OM-EGFPΔP1Δ2A < OM-EGFPΔP1. These results may be also because the defect in $2A^{pro}$ suppresses the viral replication activity and/or the expression of foreign mRNA.

ACKNOWLEDGMENTS

We are grateful to T. Matano, N. Kamoshita, A. Yanagiya, and N. Matsuda for suggestions and discussions. We also thank A. Ohmura for technical support and E. Suzuki for help in preparing the manuscript. We are grateful to C. D. Morrow for generously providing VV-P1.

This work was supported in part by Grants-in-Aid for Advanced Medical Science Research by Ministry of Education, Culture, Sports, Science and Technology (MEXT), a Grant-in-Aid for Scientific Research on Priority Areas, a Grant-in-Aid for Scientific Research (S), a Grant-in-Aid for Scientific Research on Priority Areas, a Grant-in-Aid for Young Scientists (B), a Health Labor Sciences Research Grant, special coordination funds for promoting Science and Technology, contracted research allowance "Research and Development in a New Converting Field Based on Nanotechnology and Materials Science" by MEXT, and The Naito Foundation.

REFERENCES

1. **Agol, V. I., G. A. Belov, K. Bienz, D. Egger, M. S. Kolesnikova, N. T. Raikhlin, L. I. Romanova, E. A. Smirnova, and E. A. Tolskaya.** 1998. Two types of death of poliovirus-infected cells: caspase involvement in the apoptosis but not cytopathic effect. Virology **252:**343–353.
2. **Agol, V. I., G. A. Belov, K. Bienz, D. Egger, M. S. Kolesnikova, L. I. Romanova, L. V. Sladkova, and E. A. Tolskaya.** 2000. Competing death programs in poliovirus-infected cells: commitment switch in the middle of the infectious cycle. J. Virol. **74:**5534–5541.
3. **Almstead, L. L., and P. Sarnow.** 2007. Inhibition of U snRNP assembly by a virus-encoded proteinase. Genes Dev. **21:**1086–1097.
4. **Ansardi, D. C., Z. Moldoveanu, D. C. Porter, D. E. Walker, R. M. Conry, A. F. LoBuglio, S. McPherson, and C. D. Morrow.** 1994. Characterization of poliovirus replicons encoding carcinoembryonic antigen. Cancer Res. **54:** 6359–6364.
5. **Ansardi, D. C., D. C. Porter, and C. D. Morrow.** 1993. Complementation of a poliovirus defective genome by a recombinant vaccinia virus which provides poliovirus P1 capsid precursor in trans. J. Virol. **67:**3684–3690.
6. **Belov, G. A., L. I. Romanova, E. A. Tolskaya, M. S. Kolesnikova, Y. A. Lazebnik, and V. I. Agol.** 2003. The major apoptotic pathway activated and suppressed by poliovirus. J. Virol. **77:**45–56.
7. **Bodian, D.** 1955. Emerging concept of poliomyelitis infection. Science **122:** 105–108.
8. **Borman, A. M., R. Kirchweger, E. Ziegler, R. E. Rhoads, T. Skern, and K. M. Kean.** 1997. eIF4G and its proteolytic cleavage products: effect on initiation of protein synthesis from capped, uncapped, and IRES-containing mRNAs. RNA **3:**186–196.
9. **Burgon, T. B., J. A. Jenkins, S. B. Deitz, J. F. Spagnolo, and K. Kirkegaard.** 2009. Bypass suppression of small-plaque phenotypes by a mutation in poliovirus 2A that enhances apoptosis. J. Virol. **83:**10129–10139.
10. **Calandria, C., A. Irurzun, A. Barco, and L. Carrasco.** 2004. Individual expression of poliovirus 2Apro and 3Cpro induces activation of caspase-3 and PARP cleavage in HeLa cells. Virus Res. **104:**39–49.
11. **Castello, A., J. M. Izquierdo, E. Welnowska, and L. Carrasco.** 2009. RNA nuclear export is blocked by poliovirus 2A protease and is concomitant with nucleoporin cleavage. J. Cell Sci. **122:**3799–3809.
12. **Cole, C. N.** 1975. Defective interfering (di) particles of poliovirus. Prog. Med. Virol. **20:**180–207.
13. **Cole, C. N., D. Smoler, E. Wimmer, and D. Baltimore.** 1971. Defective interfering particles of poliovirus. I. Isolation and physical properties. J. Virol. **7:**478–485.
14. **Collis, P. S., B. J. O'Donnell, D. J. Barton, J. A. Rogers, and J. B. Flanegan.** 1992. Replication of poliovirus RNA and subgenomic RNA transcripts in transfected cells. J. Virol. **66:**6480–6488.
15. **Etchison, D., S. C. Milburn, I. Edery, N. Sonenberg, and J. W. Hershey.** 1982. Inhibition of HeLa cell protein synthesis following poliovirus infection correlates with the proteolysis of a 220,000-dalton polypeptide associated with eucaryotic initiation factor 3 and a cap binding protein complex. J. Biol. Chem. **257:**14806–14810.
16. **Hagino-Yamagishi, K., and A. Nomoto.** 1989. In vitro construction of poliovirus defective interfering particles. J. Virol. **63:**5386–5392.
17. **Hambidge, S. J., and P. Sarnow.** 1992. Translational enhancement of the poliovirus 5′ noncoding region mediated by virus-encoded polypeptide 2A. Proc. Natl. Acad. Sci. U. S. A. **89:**10272–10276.
18. **Hunt, S. L., T. Skern, H. D. Liebig, E. Kuechler, and R. J. Jackson.** 1999. Rhinovirus 2A proteinase mediated stimulation of rhinovirus RNA translation is additive to the stimulation effected by cellular RNA binding proteins. Virus Res. **62:**119–128.
19. **Jang, S. K., M. V. Davies, R. J. Kaufman, and E. Wimmer.** 1989. Initiation of protein synthesis by internal entry of ribosomes into the 5′ nontranslated region of encephalomyocarditis virus RNA in vivo. J. Virol. **63:**1651–1660.
20. **Jang, S. K., H. G. Krausslich, M. J. Nicklin, G. M. Duke, A. C. Palmenberg, and E. Wimmer.** 1988. A segment of the 5′ nontranslated region of encephalomyocarditis virus RNA directs internal entry of ribosomes during in vitro translation. J. Virol. **62:**2636–2643.
21. **Kajigaya, S., H. Arakawa, S. Kuge, T. Koi, N. Imura, and A. Nomoto.** 1985. Isolation and characterization of defective-interfering particles of poliovirus Sabin 1 strain. Virology **142:**307–316.
22. **Kaminski, A., M. T. Howell, and R. J. Jackson.** 1990. Initiation of encephalomyocarditis virus RNA translation: the authentic initiation site is not selected by a scanning mechanism. EMBO J. **9:**3753–3759.
23. **Kolupaeva, V. G., I. B. Lomakin, T. V. Pestova, and C. U. Hellen.** 2003. Eukaryotic initiation factors 4G and 4A mediate conformational changes downstream of the initiation codon of the encephalomyocarditis virus internal ribosomal entry site. Mol. Cell. Biol. **23:**687–698.
24. **Kuechler, E., J. Seipelt, H. D. Liebig, and W. Sommergruber.** 2002. Picornavirus proteinase-mediated shutoff of host cell translation: direct cleavage of a cellular initiation factor, p. 301–311. *In* B. L. Semler and E. Wimmer (ed.), Molecular biology of picornaviruses. ASM Press, Washington, DC.
25. **Kuge, S., I. Saito, and A. Nomoto.** 1986. Primary structure of poliovirus defective-interfering particle genomes and possible generation mechanisms of the particles. J. Mol. Biol. **192:**473–487.
26. **Lawson, M. A., and B. L. Semler.** 1990. Picornavirus protein processing—enzymes, substrates, and genetic regulation. Curr. Top. Microbiol. Immunol. **161:**49–87.
27. **Li, X., H. H. Lu, S. Mueller, and E. Wimmer.** 2001. The C-terminal residues of poliovirus proteinase 2A(pro) are critical for viral RNA replication but not for cis- or trans-proteolytic cleavage. J. Gen. Virol. **82:**397–408.
28. **Lundquist, R. E., M. Sullivan, and J. V. Maizel, Jr.** 1979. Characterization of a new isolate of poliovirus defective interfering particles. Cell **18:**759–769.
29. **Molla, A., S. K. Jang, A. V. Paul, Q. Reuer, and E. Wimmer.** 1992. Cardioviral internal ribosomal entry site is functional in a genetically engineered dicistronic poliovirus. Nature **356:**255–257.
30. **Molla, A., A. V. Paul, M. Schmid, S. K. Jang, and E. Wimmer.** 1993. Studies on dicistronic polioviruses implicate viral proteinase $2A^{pro}$ in RNA replication. Virology **196:**739–747.
31. **Nomoto, A., B. Detjen, R. Pozzatti, and E. Wimmer.** 1977. The location of the polio genome protein in viral RNAs and its implication for RNA synthesis. Nature **268:**208–213.
32. **Omata, T., H. Horie, S. Kuge, N. Imura, and A. Nomoto.** 1986. Mapping and sequencing of RNAs without recourse to molecular cloning: application to RNAs of the Sabin 1 strain of poliovirus and its defective interfering particles. J. Biochem. **99:**207–217.

33. **Pelletier, J., and N. Sonenberg.** 1989. Internal binding of eucaryotic ribosomes on poliovirus RNA: translation in HeLa cell extracts. J. Virol. **63:**441–444.
34. **Pelletier, J., and N. Sonenberg.** 1988. Internal initiation of translation of eukaryotic mRNA directed by a sequence derived from poliovirus RNA. Nature **334:**320–325.
35. **Pestova, T. V., C. U. Hellen, and I. N. Shatsky.** 1996. Canonical eukaryotic initiation factors determine initiation of translation by internal ribosomal entry. Mol. Cell. Biol. **16:**6859–6869.
36. **Porter, D. C., D. C. Ansardi, W. S. Choi, and C. D. Morrow.** 1993. Encapsidation of genetically engineered poliovirus minireplicons which express human immunodeficiency virus type 1 Gag and Pol proteins upon infection. J. Virol. **67:**3712–3719.
37. **Porter, D. C., L. R. Melsen, R. W. Compans, and C. D. Morrow.** 1996. Release of virus-like particles from cells infected with poliovirus replicons which express human immunodeficiency virus type 1 Gag. J. Virol. **70:**2643–2649.
38. **Sabin, A. B.** 1956. Pathogenesis of poliomyelitis: reappraisal in the light of new data. Science **123:**1151–1157.
39. **Shiroki, K., T. Ishii, T. Aoki, M. Kobashi, S. Ohka, and A. Nomoto.** 1995. A new cis-acting element for RNA replication within the 5′ noncoding region of poliovirus type 1 RNA. J. Virol. **69:**6825–6832.
40. **Tobin, G. J., D. C. Young, and J. B. Flanegan.** 1989. Self-catalyzed linkage of poliovirus terminal protein VPg to poliovirus RNA. Cell **59:**511–519.
41. **Tolskaya, E. A., L. I. Romanova, M. S. Kolesnikova, T. A. Ivannikova, E. A. Smirnova, N. T. Raikhlin, and V. I. Agol.** 1995. Apoptosis-inducing and apoptosis-preventing functions of poliovirus. J. Virol. **69:**1181–1189.
42. **Weidman, M. K., R. Sharma, S. Raychaudhuri, P. Kundu, W. Tsai, and A. Dasgupta.** 2003. The interaction of cytoplasmic RNA viruses with the nucleus. Virus Res. **95:**75–85.
43. **Yanagiya, A., Q. Jia, S. Ohka, H. Horie, and A. Nomoto.** 2005. Blockade of the poliovirus-induced cytopathic effect in neural cells by monoclonal antibody against poliovirus or the human poliovirus receptor. J. Virol. **79:**1523–1532.
44. **Yogo, Y., and E. Wimmer.** 1972. Polyadenylic acid at the 3′-terminus of poliovirus RNA. Proc. Natl. Acad. Sci. U. S. A. **69:**1877–1882.
45. **Ziegler, E., A. M. Borman, F. G. Deliat, H. D. Liebig, D. Jugovic, K. M. Kean, T. Skern, and E. Kuechler.** 1995. Picornavirus 2A proteinase-mediated stimulation of internal initiation of translation is dependent on enzymatic activity and the cleavage products of cellular proteins. Virology **213:**549–557.

FEBS Letters 583 (2009) 213–218

FEBS Letters

journal homepage: www.FEBSLetters.org

Silencing efficiency differs among tissues and endogenous microRNA pathway is preserved in short hairpin RNA transgenic mice

Hiroki Sasaguri [a,c], Tasuku Mitani [b], Masayuki Anzai [b], Takayuki Kubodera [a,c], Yuki Saito [a], Hiromi Yamada [a], Hidehiro Mizusawa [a,c], Takanori Yokota [a,*]

[a] Department of Neurology and Neurological Science, Graduate School, Tokyo Medical and Dental University, 1-5-45 Yushima, Bunkyo-ku, Tokyo 113-8519, Japan
[b] Institute of Advanced Technology, Kinki University, 14-1 Minami-Akasaka, Kainan, Wakayama 642-0017, Japan
[c] Twenty-First Century Center of Excellence Program on Brain Integration and Its Disorders, Tokyo Medical and Dental University, 1-5-45 Yushima, Bunkyo-ku, Tokyo 113-8519, Japan

ARTICLE INFO

Article history:
Received 28 August 2008
Revised 20 November 2008
Accepted 1 December 2008
Available online 11 December 2008

Edited by Ulrike Kutay

Keywords:
RNA interference
Short hairpin RNA
Small interfering RNA
Transgenic mice
MicroRNA
Oversaturation

ABSTRACT

In short hairpin RNA (shRNA) transgenic mice, the tissue difference in gene silencing efficiency and oversaturation of microRNA (miRNA) pathway have not been well assessed. We studied these problems in our previously-reported anti-copper/zinc superoxide dismutase (SOD1) shRNA transgenic mice. Although there was a tissue difference (liver and skeletal muscle, >95%; central nervous system and lung, ~80%), the target gene silencing was systemic and our anti-SOD1 shRNA transgenic mice recapitulated the SOD1-null mice. Neither endogenous miRNAs nor their target gene levels were altered, indicating the preservation of endogenous miRNA pathways. We think that the shRNA transgenic mice can be utilized for gene analysis.

1. Introduction

RNA interference (RNAi) is evolutionally conserved sequence-specific post-transcriptional gene silencing, which is mediated by small double stranded RNA (dsRNA) [1]. The long dsRNA is cleaved by an RNase III enzyme, Dicer, in cytoplasm to generate small interfering RNA (siRNA) that is 21–23 base pair dsRNA. The target mRNA is recognized by guide (antisense) strand of the dsRNA in RNA-induced silencing complex (RISC), and is cleaved by Argonaute-2 (Ago2) protein, one of the main components of RISC [2]. This post-transcriptional gene silencing can be effectively induced by exogenously introduced siRNA or intracellularly expressed short hairpin RNA (shRNA) in mammalian cells [2,3].

The shRNA transgenic mice have been published [4–7] and expected to be an alternative method to the conventional knockout mice. For using shRNA transgenic mice as a tool for gene analysis in vivo, we need to know difference in silencing efficiency among tissues. Moreover, in shRNA transgenic mice, it is also important to elucidate whether microRNA (miRNA) is normally processed, because shRNA and miRNA share intracellular machineries for their maturation in mammalian cells [8–10]. We had generated anti-mouse copper/zinc superoxide dismutase (SOD1) shRNA transgenic mice, in which shRNA was ubiquitously expressed by the RNA polymerase III (Pol III) promoter [11]. Using these mice, we here evaluated the silencing efficiency in various tissues and studied endogenous miRNA pathway.

Abbreviations: shRNA, short hairpin RNA; miRNA, microRNA; RNAi, RNA interference; dsRNA, double stranded RNA; RISC, RNA-induced silencing complex; Ago2, Argonaute-2; SOD1, copper/zinc superoxide dismutase; Pol III, polymerase III; ES, embryonic stem; PBS, phosphate-buffered saline; SDS, sodium dodecyl sulfate; cDNA, complementary DNA; RT-PCR, reverse transcription polymerase chain reaction; GAPDH, glyceraldehyde-3-phosphate dehydrogenase; snRNA, small nuclear RNA; AAV, adeno-associated virus

* Corresponding author. Fax: +81 3 5803 0169.
E-mail address: tak-yokota.nuro@tmd.ac.jp (T. Yokota).

2. Materials and methods

2.1. Generation of anti-SOD1 shRNA transgenic mice

All experiments were approved by the Animal Experiment Committees of Tokyo Medical and Dental University (#0090104) and Kinki University (KAAT-19-006). We generated an anti-SOD1

0014-5793/$34.00
doi:10.1016/j.febslet.2008.12.012

shRNA expression vector and anti-SOD1 shRNA transgenic mice as reported previously [11,12]. In brief, we inserted anti-SOD1 shRNA driven by human U6 promoter into pUC19 (Takara). The shRNA expression vector was introduced into the 129/Sv embryonic stem (ES) cells (Chemicon) by electroporation. The ES cell clones in which SOD1 protein levels were effectively suppressed were introduced into C57BL/6 blastocysts (CLEA) by microinjection. We obtained F1 transgenic mice by crossing the chimeric male mice with wild-type C57BL/6 female mice.

2.2. Histological study

To analyze hepatic lipid accumulation, liver samples from 8-month-old shRNA transgenic male mice and wild-type littermates were sectioned (4 μm) and fixed in 4% paraformaldehyde/phosphate-buffered saline (PBS) for 5 min, and then stained with filtrated Sudan III (Muto pure chemicals) at 37 °C for 30 min. Counterstaining of nuclei was performed with Mayer hematoxylin solution (Muto pure chemicals) for 3 min.

2.3. Western blot analysis

Western blot analysis was performed as reported previously [11]. Mice were killed under anesthesia with pentobarbital sodium, and perfused with cold PBS. Tissues were homogenized in the cold buffer containing 0.1% sodium dodecyl sulfate (SDS), 1% sodium deoxycholate, 1% Triton X-100, 1 mM phenylmethylsulfonyl fluoride and protease inhibitor cocktail (Sigma). Equal amounts of protein from each sample were loaded in the assays. The separated proteins were detected by specific primary antibodies; rabbit anti-SOD1 antibody (1:5000, StressGen Biotechnologies), mouse anti-β-tubulin antibody (1:1000, BD Biosciences), mouse anti-Actin antibody (1:1000, Santa Cruz Biotechnology), mouse anti-Ago2 antibody (1:500, Abcam), or rabbit anti-N-ras antibody (1:500, Santa Cruz Biotechnology).

2.4. Northern blot analysis

Northern blot analysis was performed as reported previously [11]. Ten micrograms of total RNA from each sample were loaded in the assays. The DNA probes which were used to detect RNAs were as follows; complementary DNA (cDNA) (bases 15–495) for mouse SOD1; cDNA (bases 300–614) for mouse glyceraldehyde-3-phosphate dehydrogenase (GAPDH); 5′-GGTGGAAATGAAGAAAGTAC-3′ for anti-SOD1 siRNA guide strand; 5′-ACTATACAACCTACTACCTCA-3′ for mouse let-7a; 5′-GGCATTCACCGCGTGCCTTA-3′ for mouse miR-124a; 5′-AAATATGGAACGCTTCACGA-3′ for mouse U6 small nuclear RNA (snRNA).

2.5. Quantitative reverse transcription polymerase chain reaction (RT-PCR)

After treating with TURBO DNA-free (Ambion) to remove residual genomic DNA, 1 μg of total RNA from each sample was reversely transcribed to cDNA using SuperScript III Reverse Transcriptase (Invitrogen). The cDNA was used for quantitative PCR with TaqMan system using the ABI Prism 7700 Sequence Detection System (Applied Biosystems) according to the manufacturer's protocol. The primers and probe used to quantify mouse SOD1 were 5′-GGTGCAGGGAACCATCCA-3′ for forward primer, 5′-CCCATGCTGGCCTTCAGT-3′ for reverse primer, and 5′-AGGCAAGCGGTGAACCAGTTGTGTTG-3′ for probe. The primer and probe sets of mouse GAPDH, N-ras and N-myc were purchased from Applied Biosystems. GAPDH was used to normalize the quantitative RT-PCR values.

2.6. Laser microdissection and RNA extraction from motor neurons and non-neuronal cells

Collection of motor neurons and non-neuronal cells was performed as reported previously [13]. Spinal cords of the transgenic mice or wild-type littermates were removed and embedded in Tissue-Tek O.C.T. Compound (Sakura Finetek). Seven micrometer thick sections were mounted on a MembraneSlide (Leica) and stained with HistoGene staining solution (Arcturus). Approximate one thousand motor neurons and neighboring non-neuronal cells were dissected from the ventral horn of the lumbar spinal cord for each mouse using an AS LMD system (Leica). Total RNA was extracted using RNeasy Micro Kit (Qiagen) according to the manufacturer's protocol.

2.7. Subcellular fractionation

Subcellular fractionation was performed as described previously [14]. The cerebrum or liver was gently homogenized in cold buffer (0.22 M D-mannitol, 0.07 M sucrose, at 1 mg tissue/10 μl buffer) with a glass-Teflon homogenizer (30 up-and-down strokes), and centrifuged at 600×g for 10 min. The pellets were suspended with 2.2 M sucrose and centrifuged at 40000×g for 1 h. The resulting pellets were used as nuclear fraction. The supernatants generated by the first centrifugation were used as cytoplasmic fraction. Total RNA was extracted using ISOGEN (Nippon Gene) for nuclear fraction and ISOGEN-LS (Nippon Gene) for cytoplasmic fraction, respectively.

2.8. Statistical analysis

Student's *t*-test was used to evaluate difference among tissues or difference between transgenic mice and wild-type littermates. Significance was set at $P < 0.05$. To compare the expression level on Western blot or Northern blot analysis, we used NIH ImageJ to quantify the band intensity.

3. Results

3.1. Anti-SOD1 shRNA transgenic mice recapitulate SOD1-null mice

As reported previously, we obtained anti-SOD1 shRNA transgenic mice (Fig. 1A) [11]. The silencing effect of the target gene was significant on both RNA and protein levels, and was stable with age and through to the F3 generation [11]. In contrast, there was no change in the expression levels of unrelated genes including GAPDH and β-actin ($P = 0.75$ and 0.27, respectively, data not shown). The transgenic mice showed no remarkable phenotype during development. The adult mice exhibited mild fatty liver (Fig. 1B and C) and female infertility (data not shown), which were also observed in SOD1-null mice [15,16]. These findings indicate that the phenotype of the anti-SOD1 shRNA transgenic mice is similar to that of SOD1-null mice.

3.2. The siRNA-silencing efficiency differs among the tissues of the shRNA transgenic mice

We analyzed the siRNA-silencing efficiency in the various tissues of the shRNA transgenic mice. On Western blot analysis, we observed marked suppression of SOD1 protein in all the tissues examined (Fig. 2A). However, the siRNA-silencing efficiency was clearly different among the tissues; it was extremely high in the liver and skeletal muscle (>95%) and, in contrast, was relatively low in the central nervous system and lung (~80%) (Fig. 2A and B). The

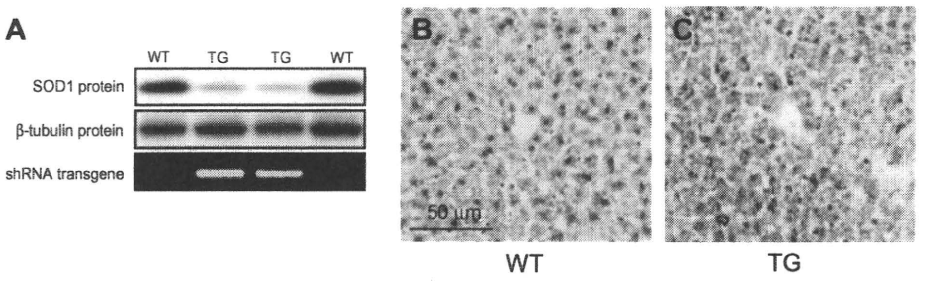

Fig. 1. Generation of anti-SOD1 shRNA transgenic mice. (A) Western blot analysis of SOD1 (upper) and β-tubulin (middle), and genomic PCR of transgene (lower) in the tails. Histological analysis in the liver of the wild-type littermates (B) and shRNA transgenic mice (C). The sections were stained with Sudan III. WT, age-matched wild-type littermates; TG, transgenic mice.

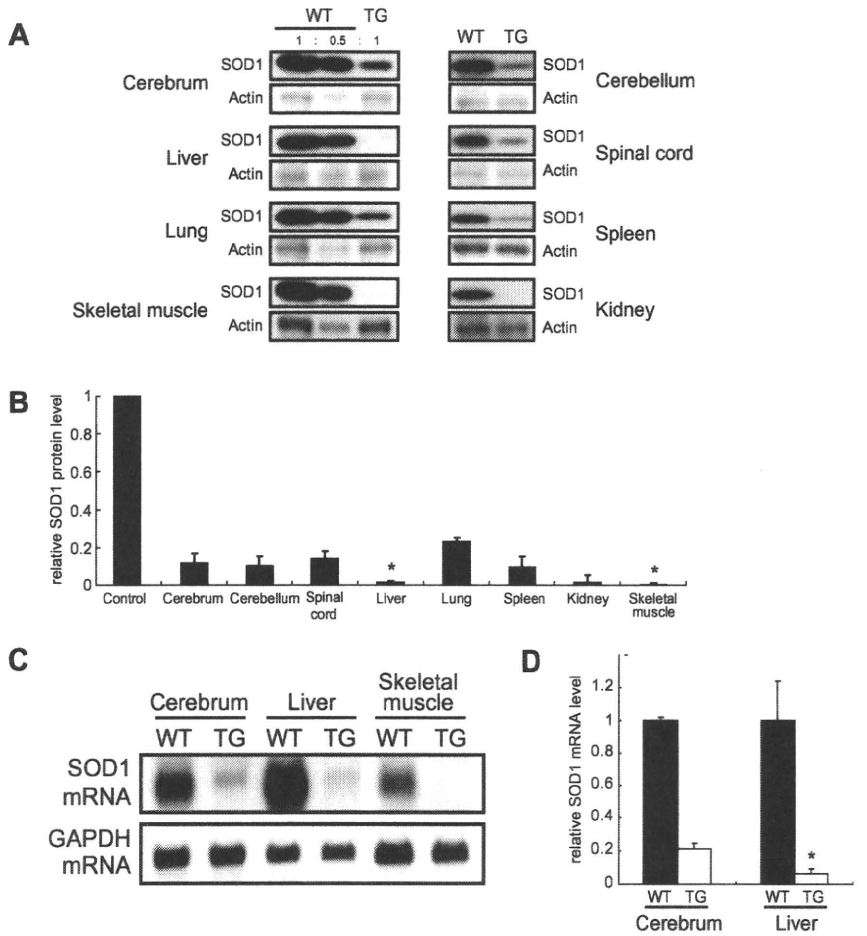

Fig. 2. Silencing efficiency in the various tissues of the shRNA transgenic mice. (A) SOD1 protein levels on Western blot analysis in the tissues of the transgenic mice. A half amounts of the wild-type samples are loaded in the middle lanes of left panel to show that the signals are not saturated. (B) Quantification of their band intensities. Values are the ratio to those of age-matched wild-type littermates (mean and S.D., $n = 3$, $^{*}P < 0.05$; significance compared to cerebrum). (C) SOD1 mRNA of the cerebrum, liver and skeletal muscle on Northern blot analysis. (D) Quantitative RT-PCR of SOD1 mRNA in the cerebrum and liver. Values are the ratio to age-matched wild-type littermates (mean and S.D., $n = 3$, $^{*}P < 0.05$; significance compared to cerebrum).

difference was also confirmed on RNA level by Northern blot analysis (Fig. 2C) and quantitative RT-PCR (Fig. 2D).

3.3. The siRNA-silencing efficiency in neuronal cells is relatively lower than those in hepatocytes and muscle fibers

Because central nervous system is composed of heterogenous cell populations, we sought to evaluate the siRNA-silencing efficiency in neuronal and non-neuronal cells using laser microdissection method. The motor neurons and non-neuronal cells were isolated from the ventral horn of the lumbar spinal cords in the shRNA transgenic mice or wild-type littermates (Fig. 3A–D), and SOD1 mRNA levels were quantified by quantitative RT-PCR. The silencing efficiency in the motor neurons was approximately 80% which was similar to the non-neuronal cells (Fig. 3E) and the whole spinal cord tissue (Fig. 2B), and was less than those in the liver and